UNH-64-6

[redacted]

Department of Physics

UNIVERSITY OF NEW HAMPSHIRE

Durham

THE UNIVERSITY OF NEW HAMPSHIRE

MAGNETOMETER PAYLOAD

by
N. C. Maynard, P. E. Lavoie
and
S. B. Marshall, III

Physics Department
University of New Hampshire
Durham, New Hampshire

Supported by the National Aeronautics and Space Administration under NASA Grant NSG 33-60 and Contract NAS5-3043.

The University of New Hampshire Magnetometer Payload

I. Introduction

In the systematic study of ground magnetic measurements the existence has been assumed of electrical currents flowing in horizontal layers in the ionosphere. The dynamo theory of ionospheric currents was proposed in 1882 by Stewart, to explain daily (S_q) variations in the earth's field. These variations are thought to result from the rotation of the earth under two current loops, one in each hemisphere, fixed in relation to the sun (Chapman and Bartels, 1940). The global ionospheric conductivity, depending on the magnetic field direction, collision frequencies, and the electron density, together with the global pattern of tidal winds, determines the resulting current density. The most probable altitude for these currents is in the E region between 100 and 150 km, where the various components of the conductivity tensor have their maxima.

An enhancement of the S_q current system known as the equatorial electrojet occurs near the magnetic dip equator. It is caused by an increase in effective conductivity due to Hall polarization of the ionosphere when the magnetic field is horizontal. Although the horizontal distribution of ionospheric current can be deduced from ground measurements, the

Table of Contents

vertical distribution can be determined only by rocket measurements. Rocket measurements of the currents are made by precise measurements of the magnetic field that they produce (Vestine et al, 1947; Chapman, 1954). The first direct measurements of the earth's field with rocket magnetometers were made by Singer, Maple, and Bowen (1951). Subsequent measurements have been made by Cahill and Van Allen, 1958; Cahill, 1959; Heppner et al, 1958; Conley, 1960; Hutchinson and Shuman, 1961; Burrows and Hall, 1965; Davis et al, 1965. A comparison of techniques for rocket-borne measurements can be found in the "Technique Manual for Ionospheric Current Measurements," (Cahill, 1964).

The University of New Hampshire rocket magnetometer experiment was designed to study the S_q current system and the equatorial electrojet. The magnetic field was measured with a nuclear free precession magnetometer, and electron density was monitored with a DC Langmuir probe. The Nike-Apache two-stage solid fuel rocket was chosen for the vehicle. It can reach an apogee of about 170 km with a sixty-pound payload -- well above the expected range of the currents, yet not so high that the region of interest (90 to 150 km) is passed through too quickly. Flights have been made to measure S_q currents at Wallops Island, Virginia (1963), and off the coast of Peru (1965), (Maynard and Cahill, 1965b). Measurements of the equatorial electrojet have been made over India (1964) (Maynard et al, 1965; Maynard and Cahill, 1965a), and off the coast of Peru (1965), (data analysis now in progress).

II. Payload Design

A. General

The UNH rocket magnetometer payload consists of the two main experiments, the proton magnetometer and the Langmuir probe, and three supporting experiments, a barometric pressure switch and a radiation chamber densitometer (measuring air pressure) for trajectory determination, and a magnetic aspect sensor for rocket aspect information. A block diagram of the payload is found in Figure 1.

The signal from the magnetometer sensor is amplified and fed directly to the mixer for telemetering to the ground. The magnetic aspect sensor modulates a 22-kc subcarrier oscillator (SCO), while the densitometer information modulates a 40 kc SCO. The baroswitch is also used to switch the Langmuir probe amplifiers from a calibration resistor to the probe. The Langmuir information is put on a 70-kc SCO channel. The signals are combined in the mixer, amplified and fed into the transmitter. Information is radioed back to ground through the circularly-polarized quadrupole antennas at the base of the payload.

In designing the physical layout of the payload (Figure 2), the prime consideration was to minimize the magnetic field from the payload at the magnetometer sensor location. A payload field less than 2γ was achieved. Each unit also had to function after large shocks and vibrations from the firing of

the rockets. The magnetometer sensor was placed as far as possible up into the nose cone to separate it from the electronics. A fiberglass deck structure and housing were used, since any conductive loops around the magnetometer coil would destroy the signal. Each experiment was mounted on one or two decks which could be plugged, as separate units, into the raceway containing the interconnecting wiring harness (Figure 3). Interchangeability of decks between payloads was desired for convenience in field operations.

B. The Proton Magnetometer

1. Theory

The proton precession magnetometer of Packard and Varian (1953), and Waters (1955), (also Waters and Francis, 1958), is easily adaptable to rocket measurements. The sensor unit is simple and rugged, and the instrument requires no in-flight calibration, since the measurement is dependent upon nuclear constants.

If a sample of liquid, rich in hydrogen nuclei, is subjected to an external polarizing magnetic field several orders of magnitude larger than the earth's magnetic field, the spin axes of the protons in the sample will be aligned along the polarizing field. Then, if the polarizing field is suddenly reduced to zero, the protons will commence to realign with the earth's field, and while so doing, will freely precess about the earth's field. A small AC voltage at the precession frequency will be induced in any coil of wire around the sample.

The earth's magnetic field is related to the precession frequency by the Larmour relationship,

$$B = \frac{2\pi f_p}{\gamma_p} \qquad (1)$$

where f_p is the precession frequency, and γ_p ($2.67523 \pm .002 \times 10^4$ radians/sec. gauss), the gyromagnetic ration of the nucleus (Driscoll and Bender, 1958). Since γ_p is known to within two parts in 10^5, measurement of the precession frequency may limit the absolute accuracy of the measurement.

The same coil can be used for signal pickup and for establishing the polarizing field. A 700-turn coil, with several amperes polarizing current, produces a precessing signal of a few microvolts. The output voltage can be expressed by

$$V = 4\pi K\ N\ A\ X\ B_0 \gamma_p\ B_e \cdot \sin^2\theta \cdot e^{-t/T^2} \sin(\gamma_p B_e t) \cdot 10^{-8} \text{volts} \quad (2)$$

(Cahill and Van Allen, 1956), where

K = geometric factor

N = number of turns

A = cross sections of sample

X = paramagnetic susceptibility of the protons

B_0 = polarizing field

γ_p = geomagnetic ratio of the proton

B_e = earth's field

θ = angle between coil axis and earth's field

T_2 = transverse relaxation time

t = time in seconds

Note that the amplitude of the signal falls off as $\sin^2\theta$; hence, if the coil is aligned with the earth's field, there will be no signal. Also, the phase coherence of the precessing nuclei will decrease in time resulting in an exponential decay of the signal. The polarize cycle must be longer than the relaxation time to allow the protons to approach complete

alignment with the polarizing field. In order to obtain a good signal, the polarization field must be removed in a time that is short compared to the period of one cycle of the precession frequency. In addition there should be no magnetic field gradients across the sample, since the resulting difference in precession frequency will destroy the coherence of the signal. A precession frequency of approximately 2000 cps is obtained in a 0.5 gauss (50,000 γ) field.

The accuracy to which the gyromagnetic ration of the proton is known allows absolute measurement to within one γ. Better relative accuracy can be obtained, depending only on precision of frequency measurement. Noise in the signal has been the limiting factor in frequency measurement with the miniature rocket magnetometer.

2. Design and Operation

A proton magnetometer designed for operation in rockets must meet the following requirements:

1. It must be able to withstand severe shock and vibration.
2. The low level (microvolt) of the precession signal demands considerable amplification to attain a volt-level signal for telemetry. The signal-to-noise ratio must be kept above two to one for precise frequency measurements.

3. The sensor magnetometer, electronics and remainder of the payload must be free from magnetic materials which would create a field at the sensor.
4. Measurements must be made as frequently as possible without sacrificing the precision of frequency determination, since the rocket is traveling more than 1 km/sec during portions of the flight.

Figure 4 depicts the block diagram of the magnetometer used on the University of New Hampshire flights. The programmer controls the relays, which alternately connect the amplifier or the polarizing supply to the sensor coil. During the polarizing period (about 0.7 sec), the polarizing batteries send a current of 4 amperes through the coil. The polarizing current is then turned off, and the coil is connected during the read period of 0.7 second, to the high gain preamplifier. The signal from the coil is amplified to the 10 millivolt level. In the tuned main amplifier the signal is amplified to 4 volts for mixing with the SCO signals and direct modulation of the FM transmitter.

a) Sensor Coil

The sensor coil (Figure 5) consists of ten layers, 70 turns each layer, of #16 wire wound on a fiberglass tube and held in place by phenolic discs. A polyethylene

sample bottle fits tightly inside the coil form. Kerosene, which has a relaxation time of about 0.7 second, is used as the sample. Water could be used, but it has a two-second relaxation time, making the repetition rate of the measurements too slow.

An electrostatic shield (Figure 6) completely encloses the coil to reduce noise pickup. This shield is made from copper-plated fiberglass board by etching away narrow strips of copper. Care must be taken to make sure that there are no complete conductive loops around the coil, as these will destroy the signal. The unit is then encased in foam and an outer protective cover.

b) Preamplifier Assembly

The electronics for the magnetometer is divided into two packages, one containing the preamplifier, programmer, and associated relays (Figure 7), and the other containing the tuned main amplifier.

The programmer is a standard astable multivibrator with the RC combinations, C_1R_2 and C_2R_3, adjusted so that the circuit will remain in each state about 0.7 second. The output from the collector of TR_2 triggers a switch (TR_3) which controls the relays.

Relay RY_1 switches the polarizing power to the coil and controls the operation of RY_2. RY_2 is used in switching the amplifier to the coil and also to supply a 220Ω resistor

across the input to the amplifier during the polarize cycle when the coil is disconnected, to prevent oscillation. Relay RY_2 is a G.E. 352791G200A5 Relay. RY_1, a Sigma 33RJ490FGSIL, was chosen for its low contact resistance, hence its ability to handle very small signals along with its high current rating (2 amps). Since it produces a strong magnetic field, it was necessary to enclose it in a MU-metal shield. A relay meeting all requirements and rated at a higher current was desirable, but it was not available. The capacitor across RY_2 delays the operation of RY_2 for about 20 milliseconds to allow suppression of transients from the switching. Contacts of RY_2 are arranged to cancel transients resulting from contact potentials in the relay.

To dissipate the inductive switching transient from the coil, a clipping network is employed across the coil. The diode CR_4, back-biased during the polarization, conducts the energy from the transient into C_4, which in turn dissipates it in R_5.

The preamplifier is a very low-noise tuned amplifier with a gain of about 3000. Because of the very low-level signal, RCA 2N220, low-noise germanium transistors were used in all three stages to keep noise generation in the amplifier itself at a minimum.

The first stage is a common emitter, transformer-coupled, tuned amplifier. The Triad TY55X (T-1) transformer is used

to match the impedance of the coil to the input impedance of TR-1. Resistor R_{16} serves to bias the emitter and limit the collector-to-emitter current to the RCA recommended value of 400 μa for lowest noise operation. Tuning is accomplished through series resonance of the secondary of T-1 and the base emitter junction capacity of TR-1. This is aided by C_{12} and R_{14}. Resistor R_{14} adjusts the bandwidth, while C_{12} shifts the frequency. For wide changes in frequency it is necessary to adjust R_8 and R_9, thus changing the biasing and therefore the junction capacity. In practice it was found best to leave out R_{14} and C_{12} during construction and to use substitution boxes to tune roughly to the desired frequency and bandwidth. Typical values for R_{14} and C_{12} are 180Ω and 0.5 μf.

Transformer T_2 is used to couple the high output impedance of TR-1 to the low output impedance of TR-2. The second stage is a grounded emitter, untuned, voltage amplifier. Capacitor C_{15} further shapes the passband and helps the signal-to-noise ratio by limiting the high frequency response of the amplifier. This also served to limit interference from the transmitter power convertor which operated at about 3200 cps.

The third stage is an emitter follower to provide low output impedance and isolation of the other stages from loading effects.

Resistor R_{10}, and Capacitors C_8 and C_4, stabilize the supply voltage to each transistor and decouple any signal

voltages appearing on the supply line that could cause feedback and oscillation. Bias for the circuit is -12v.

Printed-circuit construction was used for the circuitry, and the board was encased in foam for shock and vibration protection. A copper box covered the foamed circuit and served as an RF shield.

Wave traps were used on all signal leads entering and leaving the box to reduce RF interference. They were made from a ceramic 10-μμf capacitor with three turns of wire wrapped around (in parallel with) the capacitor. The traps were tuned to the transmitter frequency by changing the spacing between the turns. The high gain tuned amplifier was subject to oscillation when modulating the FM transmitter. The feedback apparently was through leakage of the RF signal into the circuit boxes and demodulation there. It is recommended for future flights that these traps be in all leads, power leads as well as signal leads, entering the copper box. Oscillation can also occur if the sensor coil is improperly connected to the first stage of the amplifier.

c) Main Tuned Amplifier

Figure 8 shows the schematic for the main amplifier. The four-stage amplifier was designed to amplify the output of the preamp to the 4-volt level necessary to feed into the telemetry system and to further reduce noise on the signal. Resistor R_1 controls the overall gain of the system and is used to adjust the output to the desired level for feeding into the telemetry system. Capacitor C_2 is used to limit further the high frequency response of the circuit.

The first stage (TR1) is a common emitter voltage amplifier. The output is capacitive-coupled into the second stage. The second stage is identical with the first stage with the exception of R_8. This stage is meant to be driven into saturation and cut-off to clip the signal. R_8 is used to adjust the peak voltage value of saturation and cut-off. R_6 and R_7 are adjusted to obtain symmetrical clipping. RCA 2N217 germanium transistors are used throughout.

Variations in amplitude of the output signal are effectively removed by clipping. Preservation of the amplitude of the signal is not necessary, since all the information is contained in the frequency. (The output at the collector of TR_2 should be a square wave of amplitude 2 volts, peak to peak.) The clipping lessens the effect of noise in the signal and thus effectively lengthens the useful portion of the exponentially decaying signal. Clipping continues until the precession signal has decayed below the level set by R_8, and the output will be of constant amplitude until this time.

The output of the second stage is directly coupled into TR_3, which is used in an emitter follower configuration for isolation and impedance matching into the band-pass filter. The band-pass filter, designed from equations given by Terman (1943), serves to select the fundamental frequency from the square wave and to further remove noise of frequencies outside of the band-pass region. The center frequency can best be adjusted by varying C_7 and C_9, while the band width is set by R_{12}.

In practice each adjustment will slightly affect the other. The inductors used are high Q toroidal coils manufactured by Collins Radio Company.

The final stage is an emitter follower used to provide a low output impedance and to match to the output impedance of the band-pass filter. The signal is capacitor-coupled to the telemetry system. The same power supply is used for the main amplifier as was used for the preamplifier. Large tantalum capacitors keep the supply impedance low and prevent feedback between stages and between the amplifiers. The amplifier was constructed on a printed circuit board and encased in foam inside a copper box (Figure 9). As in the preamplifier wave traps were employed on the signal leads to reduce RF interference.

3. Tuning and Associated Problems

These payloads have been flown at several different sites around the world. At each place the field is different, so the magnetometer must be tuned to the magnetic field at the launching site. The bandwidth must be wide enough to accommodate the expected field variations during flight. The UNH magnetometers have been tuned with a bandwidth of 400 cycles, and with the center of the band set to give optimum performance near the 100-km point of the flight, the region where currents are most probable.

Tuning must be done in two stages. The individual units must be tuned and then retuned when combined. The preamplifier

is tuned by inducing a variable-frequency oscillator signal in the pickup coil with one turn of wire while the coil is in a permalloy shield (to prevent 60-cycle pickup and other noise). Care must be taken to keep the input signal below 50 μa, so as not to overdrive the amplifier. For an overall bandwidth of 400 cycles, the preamplifier is adjusted to obtain a bandwidth of 600 to 700 cycles. For initial tuning of the main amplifier, a 10-mv audio-oscillator signal is introduced at the input, and the filter is adjusted as previously described to obtain the desired 400-cycle bandwidth. The units are then connected together, with the oscillator signal feeding into the coil, for a system bandwidth check. Minor adjustments may have to be made to the main amplifier filter for the desired band-pass shape. For signals in the center of the pass-band, 4 to 5 volts output is obtainable with a precession signal-to-noise-ratio of three or four to one.

As was noted in the theory of operation, gradients in the field over the dimensions of the sensor will destroy the signal. One can always check the output to be sure that it is a precession signal by holding a steel wrench next to the sensor, thus destroying the signal. For shipboard launchings the large field gradients caused by the steel hull prevent observation of the magnetometer signal until the rocket has left the launcher.

Since the majority of testing is done in Durham, some means must be created to set up a magnetic field the same as that to

be encountered in flight. Included in the University's Magnetic Field Observatory is a Fanslau coil system for establishing any field desired in the range between zero and one gauss to an accuracy of one gamma. A less elaborate, but effective, system (used to test instruments in the field) has been designed by Rubens (1945). It consists of five coils (turns ratio 19-4-9-4-19) equally spaced on a cubical coil form. If the axis of the coils is aligned with the main component of the field, the field can be canceled or strengthened to any desired level. A four-foot diameter cube is of sufficient size.

C. Langmuir Probe

1. Theory

In the early 1920's Langmuir and his colleagues developed the theory of probes protruding into a plasma (Langmuir and Mott-Smith, 1924; Mott-Smith and Langmuir, 1926). Recently, Langmuir probes have been used to investigate electron density in the ionosphere (see, for example, Smith, 1963).

In the treatment of the probe, negative and positive ions are neglected as their contribution to the probe current is negligible. The random current density to the probe, for a single probe in a plasma, may be expressed by

$$j_e = m_e \frac{e\bar{V}_e}{4} \qquad (3)$$

where m_e is the electron density

e is the electronic charge

and $\bar{V}_e$ is the mean electron velocity.

If we assume a Maxwell distribution (and thus, thermal equilibrium) for the electrons,

$$\bar{V}_e = \left(\frac{8kT_e}{m_e} \right)^{1/2} \qquad (4)$$

where

T_e is the electron temperature

m_e is the electron mass

k is the Boltzman constant.

When the probe is negative with respect to the plasma, only electrons with energies greater than the retarding potential will strike the probe. The current may be expressed by

$$j = j_e \exp \frac{eV}{kT_e} \qquad (5)$$

where V is the retarding potential.

Note that in this case the current is independent of the electrode configuration, and the slope of the current voltage characteristic is proportional to the electron temperature.

For accelerating potentials the size and shape of the electrodes becomes important. The two limiting cases are a plane where

$$j = j_e \qquad (6)$$

and a small sphere where

$$j = j_e \left(1 + \frac{eV}{kT} \right) \qquad (7)$$

For all other geometries the currents fall between these two limits. For any given configuration the current is proportional to the electron density, if we neglect changes in electron temperature.

In an actual experiment it is easier to use two probes and measure the current voltage characteristic of the pair. If the area ratio of the two probes is large, the smaller of the probes can be treated as a single probe, and the larger serves to establish a constant reference potential. To obtain

a large area ratio in rocket investigations of the ionosphere, a small tip probe is used for the small electrode, and the rocket motor housing constitutes the large electrode.

Since knowledge of the fine structure of the electron density was desired for correlation with the magnetic field measurements, the probe was kept in the DC mode as much as possible. The use of a constant DC potential on the probe is difficult to justify theoretically, but it is simple to achieve experimentally. The results agree with those obtained by other methods (Smith, 1963).

2. Design

The area of prime interest for comparison of electron density and electric current measurements (by magnetometer) was the E region of the ionosphere. In order to accommodate the expected changes of electron density in this region, two linear scales were used, covering two orders of magnitude, instead of the usual logarithmic amplifier. The probe amplifier was switched periodically between the two ranges. Since the rocket travels at speeds of greater than 1 km/sec in the lower E region, it was necessary to switch rapidly between scales to avoid losing data. A repetition rate of five cycles per second was chosen -- one tenth of a second for each scale. Since continuous measurements were desired, the amplifiers were DC coupled and had to be as free as possible from changes in the zero-level of the DC output. It was also necessary to find

a means of switching that would not change the level of the DC signal. Overall requirements of a magnetically clean payload also had to be met.

Figure 10 shows a block diagram of the Langmuir probe electronics. The multi-vibrator controls the amplifiers which feed into a common output. The signals are fed to the amplifiers from the sensor. The multi-vibrator output is scaled by a factor of eight to drive a one-shot multi-vibrator. This in turn triggers a ramp generator which applies a ramp voltage to the probe, sweeping from minus three volts to a DC level of 2.7 volts. This ramp allows measurement of the electron temperature. When the probe is negative to the plasma, the electron temperature is inversely proportional to the slope of the current voltage characteristic of the probe (equation 5).

a) Amplifiers

The circuit diagram for the amplifier deck is shown in Figure 11. The amplifiers are DC-coupled differential amplifiers similar to the one described in Transistor Circuit Design, by the staff of Texas Instruments. This amplifier was chosen for its high input impedance (250 kΩ), along with reasonable gain (100 to 150). An input of 20 to 30 millivolts from the sensing resistor provides full scale modulation of the subcarrier. Tests on the amplifier indicate DC drift to be less than 200 microvolts (μv), equivalent input voltage, and temperature stability better than 75 $\mu v/^{o}C$

equivalent input voltage.

The first stage on each side of the balanced amplifier configuration is an emitter follower to give high input impedance. The second stages are common emitter amplifiers fed by a current source in the emitter for stability. The 10 Ω potentiometer connecting the emitters is used for balancing. The output is taken between the two collectors of the second stages. Silicon transistors, 2N338, are used throughout. It was noticed that General Electric 2N338 consistently had higher gain and lower leakage, resulting in more amplifier gain and a higher input impedance. For stability in this amplifier it is necessary to keep both sides of the amplifier as nearly as possible in balance. The transistors and resistors should be in matched pairs. The one kilohm (kΩ) resistors on the side of the amplifier tied to the ground must be adjusted to match the sensing resistor used for the input to the other side. Since the two amplifiers are tied together in parallel, the collector resistors in the second stages are twice the optimum value for the circuit.

b) Switching

Switching between the amplifiers is accomplished by using the multivibrator to switch on and off the bias to the current generators in the amplifiers. The multivibrator is a standard astable circuit similar to that used in the programmer of the magnetometer. Each side of the multivibrator drives an emitter follower used as a current switch to apply

the bias to the amplifiers. This type of switching results in no DC level change, since the amplifier is completely off when not in use.

c) Ramp Generation

Figure 12 shows Deck 2 of the Langmuir probe electronics containing the circuitry for generation of the ramp and the sensing resistors. The output from the multivibrator is channeled into the scalers where it is scaled by a factor of eight. The scalers are bistable multivibrators in which diode steering insures that the incoming pulse will go to the proper transistor for the switching to occur. The scaled output triggers a one-shot multivibrator. The signal is then fed through an emitter follower into the ramp generator. This circuit depends on the slope of an exponential charging characteristic being nearly linear over a short range. The resulting ramp is inverted in the last stage and applied to the probe. The 5 kΩ potentiometer serves to adjust the amplitude of the ramp.

d) Sensor

The expected probe current and the voltage desired at the input of the amplifiers determine the sensing resistors. The maximum probe current during the flight in the E region is about 30 microamperes (μa). The two ranges were set for 0 to 5 μa and for 0 to 50 μa. The maximum voltage drop across the sensing resistor in each case must be enough to cause the amplifier to modulate the subcarrier fully. A 10 kΩ

resistor with 5 μa current will establish a 50 mv signal for the amplifier. Note that this is well below the 250 k input impedance of the amplifier, so no appreciable loading will occur. The sensing resistors are Corning type C, 2% glass resistors.

e) Probe

A detailed view of the Langmuir probe at the top of the payload is shown in Figure 13. The nose cone for the payload was necessarily made of fiberglass. To obtain a well-defined geometry and a large electric area ratio, it was decided to place (adjacent to the nose tip electrode) a stainless steel ring electrically connected with the payload base and rocket motor. The steel ring was separated by one inch of Teflon from the tip probe. A coaxial cable was used to bring the electrodes to the electronics package in the payload.

f) Baroswitch

Since the DC amplifier is inherently subject to drift, it was desired to provide a means of in-flight calibration. It was also useful as a check of the densitometer altimeter to provide a determination of the time the rocket passed a given altitude on the upward and downward legs of the flight. Both objectives were accomplished with the use of a barometric pressure switch set at 70,000 feet. The baroswitch used was a College Hill Industries Model 6617A, modified by the factory to make it magnetically clean. A 499 KΩ , 1% Corning type N resistor was placed between the probe and the

rocket ground, and it was removed from the circuit at 70,000 feet by the baroswitch operation. This allowed a check of the pre-flight calibration on both the upward and downward legs.

D. Associated Experiments

An ionization chamber densitometer was employed to provide an alternate means of trajectory determination. An NRC type 8717 Alphaton digital pressure transducer was modified to obtain higher pulse rate and therefore better accuracy when the pressure is changing rapidly (Figure 3). The instrument consists of an ionization chamber, containing a radioactive source and an electrometer, in a blocking oscillator circuit. At low pressures the number of molecules ionized in the chamber is small, resulting in a small electrometer current and a small pulse rate. At higher pressures the pulse rate increases as more current is detected by the electrometer tube.

Figure 14 shows the modified circuit. L_1 and R_1 were inserted to change the pulse frequency. The voltage on the chamber was also lowered to 30 volts. Other modifications were found to have a greater effect on the frequency; however, they resulted in circuit instabilities. The values used for L_1 and R_1 varied with each unit, as the circuit was very sensitive to the gain of the electrometer and the β of the transistor. R_4, C_1 and C_2 were used to shape the output pulses for the subcarrier oscillator. Wave traps (described in the magnetometer section) were used to reduce RF interference.

Also included in the payload was a magnetic aspect sensor (Heliflux magnetic aspect sensor type RAM-5C, made by the Schonstedt Instrument Company). The unit is designed to monitor one component of the field -- along the axis of the sensor. The sensor was mounted with its axis perpendicular to the spin

axis of the rocket, hence also perpendicular to the axis of the polarizing field. Thus, the axial magnetic field generated in the magnetometer coil would not affect the transverse component measurement of the aspect senscr. Figure 15 shows the aspect deck with the sensor on the right, the aspect sensor electronics on the left, and the baroswitch at the bcttom. The output of the sensor is a sine wave at the spin frequency of the rocket. Precession of the rocket is measured by noting the changes in amplitude of the sine wave, as the spin axis changes its angle with the earth's field.

E. Telemetry

An FM-FM telemetry system was employed to send the information back to the ground. Information from the Langmuir probe, aspect sensor, and densitometer modulated three voltage-controlled oscillators (Dorsett Model 018D-3). These were equipped with non-magnetic aluminum cases.

The output of the subcarriers and the magnetometer signal are combined in the mixer (Figure 16). As the Langmuir probe reference potential is not at the rocket common ground potential, the 70-kc SCO circuit is floating and operates from a separate battery. Transformer coupling is necessary at the mixer. The 70-kc signal is then fed through a common base amplifier before mixing with the other signals. The 50-kΩ, potentiometer provides additional adjustment of the magnetometer signal. The 47-kΩ resistors in the input of the SCO's are necessary to provide the proper loading impedance for the oscillators. The resulting composite signal is amplified in a common emitter circuit and passed through an emitter follower stage to lower the output impedance. Composite signal level is adjested by the 10-kΩ potentiometer.

The transmitter used was a Bendix TXV 13. The composite signal was introduced into a compensated phase modulation input. This provided a reasonably flat modulation vs. frequency characteristic. Lower frequencies required slightly more input level than did higher frequencies for the same output level. Plate voltage for the transmitter tubes was

supplied by a Sun-Air power supply. A Zener diode was placed across the output of the supply to regulate the voltage and prevent transient voltages from damaging the transmitter. The transmitter and power converter were mounted in the base antenna section, while the SCO's and the mixer were above on a separate deck. (Figure 2).

F. Power

Since not all payload circuits were at a common ground potential, it was desirable to use separate sources of power. Silver cells (Yardney HR-3NM) supplied the power for polarizing the magnetometer coil and for the power converter supplying the transmitter. Mercury cells mounted in a separate pack on the SCO deck supplied power to the Langmuir electronics. One battery deck consisted of mercury cells for the magnetometer electronics supply, an alkaline 28-volt pack for the SCO supply, mixer and aspect sensor, and a separate 30-volt battery for the 70-kc (Langmuir) SCO. Densitometer batteries were in a separate pack in the densitometer enclosure.

For safety reasons it was required that no payload power be on while the assembled rocket was being mounted on the launcher. It was necessary, therefore, to have a means of holding power off until flight. Magnetic latching relays were not desirable due to large stray magnetic field. However, it was possible to effect an electrical latch by using one of the set of contacts on the power control relay. Figure 17 shows a schematic of the main battery deck. The hold current was supplied by Yardney, HR-1NM, silver cells on the silver cell deck. A turn-on pulse to the T relays causes the hold current to be applied to all the relays except the X relays which turn on payload power. A turn-off pulse to the X relays causes the hold current to be broken, and the power to the payload to be turned off. All the relays are

GE 3S2791G200A5 "postage stamp" relays. They have a very low external field in the "on" state and were placed back-to-back for cancellation of any magnetic dipole movement. Throughout the power control circuits two relays were used in parallel to prevent accidental dropout during flight.

III Testing

Testing of the payload divided into three main phases:

1. Magnetic field tests.
2. Shock and vibration tests.
3. Individual unit and complete payload.

Although operation under extreme temperature conditions was not a prime design consideration in the instruments due to the short time of fight (about six and a half minutes), thermal tests were made on all the units, and temperature effects were minimized where possible.

A. Magnetic field tests.

In order that fields from the vehicle would not distort the ambient field to be measured, magnetic fields due to the payload were kept small. Tests of each payload deck were made in the University of New Hampshire magnetic test facility. Zero field was first established (to within 1 γ). The instrument was then passed under a three-axis flux-gate magnetometer sensor. The outputs of the magnetometer were recorded (Figure 18), on an oscillograph. At the distance of closest approach of the instrument to the magnetometer, the vector field of the tested instrument can be determined. For example, the record in Figure 18 is interpreted as an indication of a 5-gamma field due to a permanent dipole moment oriented along the X axis of the instrument. It was found that even the Subminax coaxial cable supplied as antenna

harness produced a stray field (due to its steel center conductor), and it was replaced with a copper-conductor coaxial cable. A final check of the completed payload was made after "degaussing." Payload fields were kept to less than 2 γ .

B. Shock and vibration tests

The instruments must withstand 15 to 20 G vibration, and over 50 G shocks. Initial tests were made by dropping the payload onto a pad; the acceleration was measured by a miniature accelerometer mounted on the payload. This is not convenient for routine tests of subassemblies. An effective rough check is to slam the deck down on a lab bench several times; if it does not function after this test , then a more sturdy mounting is needed. Vibration tests of a complete payload were accomplished on a shake table.

C. Individual unit and complete payload performance checks.

Each unit was individually tested and calibrated for performance of its proper function. It was also necessary to test each unit assembled in the payload with the other instruments running. Interference problems, especially RF interference, can be present. RF interference in the magnetometer and the densitometer was effectively reduced by the copper boxes and the wave traps.

A complete check of all instrumentation through telemetry was done before each payload was packed for shipment to the launch area. At the launch area further tests through the

telemetry were made before final assembly. At the time of final assembly screws and nuts were cemented in place, and "RTV" compound was applied to all wiring harnesses for strain distribution. One short final check of payload operation was made while the rocket was horizontal on the launcher. From the time of final assembly to launch, the battery voltages were monitored through the umbilical cord at the test box. This box was also used to turn power off and on in the rocket.

IV Data Handling

Recorded along with the video output of the tracking receivers was a 100-kc standard signal. This was necessary for use with the magnetometer data, as a reference standard for the frequency counter in the data reduction equipment (Figure 19). Since switching transients occur at the beginning of each magnetometer signal, the first few cycles of signal were discarded. This was done with the aid of a "dual preset" counter. The Muirhead frequency analyser served as a very narrow band filter to select the precession signal from the complex video output and to reduce noise. A passband Q value of 150 is obtainable. Rough checks of flight time were made, using the head phones to monitor the intercom channel on the flight tape.

Data from the subcarriers were removed from the flight tape with the equipment shown in Figure 20. The discriminators selected their respective signals, and this information, together with the Muirhead filter output was recorded on a Honeywell Visicorder, high-speed oscillorgraph. It was necessary to calibrate the 70-kc discriminator, since the Langmuir probe information is contained in a varying DC level. The time code from the flight tape was also on the oscillograph to provide a precise determination of the time of each measurement.

Acknowledgements

The authors wish to acknowledge the work of William B. Dickinson of the UNH Physics Department on the design of the magnetometer preamplifier. The contributions of Andrew White and Paul G. Amazeen of the Physics Department at various stages of the evolution of the final payload, and the advice of Karl Flanders on mechanical problems were appreciated.

We also wish to thank Dr. Laurence J. Cahill, Jr., under whose direction this project was carried out.

This work was supported by NASA Grant NSG 33-60 and Contract NAS5-3043.

References

Burrows, K and S. H. Hall, Rocket measurements of the geomagnetic field above Woomera, South Australia, J. Geophys. Res., 70, 2149-2152, 1965.

Cahill, L.J., Jr., Investigation of the equatorial electrojet by rocket meagnetometer, J. Geophys. Res. 64, 489-503, 1959.

Cahill, L.J., Jr., Technique for ionosphere current measurements, pub. NASA for COSPAR Work Group II for IQSY, 1964.

Cahill, L.J.,Jr., and J.A. Van Allen, High altitude measurements of the earth's magnetic field with a proton precession magnetometer, J. Geophys. Res., 61, 547-558, 1956.

Cahill, L.J., Jr., and J. A. Van Allen, New rocket measurements of ionospheric currents near the geomagnetic equator, J. Geophys. Res., 63, 270-273, 1958.

Chapman, S., Rockets and magnetic exploration of the ionosphere, Rocket Exploration of the Upper Atmosphere, R.L. Boyd and M.J. Seaton (editors) Pergammon Press, London, 292-305, 1954.

Chapman, S. and J. Bartels, Geomagnetism, Oxford University Press, 2 Vol., Chap 23, 1940.

Conley, J. M., Earth's main field to 152 kilometers above Fort Churchill, J. Geophys. Res., 65, 1074, 1960.

Davis, T.N., J.D. Stolarik, and J. P. Heppner, Rocket measurements of S_q currents at mid-latitudes, Tech. Rpt. X-612-65-226, Goddard Space Flight Center, 1965.

Driscoll, R.L. and P.L. Bender, Gyromagnetic ratio of Proton redetermined, N.B.S. Tech. News Bull. 42, 217-219, 1958.

Heppner, J.P., J.D. Stolarik and L.H. Meredith, The earth's Magnetic field above WSPG, New Mexico, from rocket measurements, J. Geophys. Res., 63, 277-288, 1958.

Hutchinson, R. and B. Shuman, Rocket measurements of the magnetic field above New Mexico, J. Geophys. Res. 66, 2687-2693, 1961.

Langmuir, I. and H.M. Mott-Smith, Studies of electric discharges in gases at low pressures, G. E. Review, 27, 449-455, 538-548, 616-623, 762-771, 810-820, 1924.

Maynard, N.C. and L.J. Cahill, Jr., Measurement of the equatorial electroject over India, sub. J. Geophys. Res. June, 1965.

Maynard, N.C. and L.J. Cahill, Jr., Preliminary results of measurements of S_q currents and the equatorial electroject near Peru, sub. to J. Geophys. Res. as Letter to the Editor, August, 1965.

Maynard, N.C., L.J. Cahill, Jr., and T.S.G. Sastry, Preliminary results of measurements of the equatorial electroject over India, J. Geophys. Res., 70, 1241-1245, 1965.

Mott-Smith, H.M. and I. Langmuir, The theory of collectors in gaseous discharges, Phys. Rev., 28, 727-763, 1926.

Packard, M. and R. Varian, Free nuclear induction in the earth's magnetic field, Phys. Rev., 93, 341, 1954.

Rubens, S.M., Cube-surface coil for producing a uniform magnetic field, Review of Sci. Inst., 16, 243-245, 1945.

Singer, S.F., E. Maple, and W.A. Bowen, Jr., Evidence for ionospheric current from rocket experiments near the geomagnetic equator, J. Geophys. Res., 56, 265-281, 1951.

Smith, L.G., A DC probe for rocket measurements in the ionosphere, Geophys. Corp. Am. Tech. Rpt., 63-19-N, June, 1963.

Staff of Texas Instruments, Transistor Circuit Design, 1963. Chap. 8, McGraw Hill, 1963.

Stewart, B., Terrestrial magnetism, Encyclopedia Britannica, 9th ed., 36 pp., 1882.

Terman, F.E., Radio Engineers Handbook, McGraw Hill, 1943.

Vestine, E.H., L. La Port, I. Lange, and W.E. Scott, The Geomagnetic field -- description and analysis, Carnegie Institution of Washington, Publ., 580, 1947.

Waters, G.S., A measurement of the earth's magnetic field by nuclear induction, Nature, 176, 691, 1955.

Waters, G.S. and P.D. Francis, A nuclear magnetometer, J. of Sci. Inst., 35, 88-93, 1958.

Figure 1. Block diagram of the UNH rocket magnetometer payload.

Figure 2. Picture and layout diagram of the payload showing the location of each major instrument.

Figure 3. Photograph of the densitometer unit mounted on the antenna base section. The photograph also shows the bottom of the raceway with Cannon connectors for each deck.

Figure 4. Block diagram of the UNH proton precession magnetometer.

Figure 5. Photograph of the sensor coil showing it in its various stages of construction.

Figure 6. Drawing of the electrostatic shield used to encase the sensor coil for reduction of noise pickup.

Figure 7. Schematic of the preamplifier unit showing the preamplifier, programmer, associated relaying and the clipping network.

Figure 8. Schematic of the main tuned amplifier.

Figure 9. Picture showing construction details of the main amplifier unit.

Figure 10. Block diagram of the Langmuir probe electronics.

Figure 11. Circuit diagram of the Langmuir probe amplifier deck showing the amplifiers and the multivibrator programmer.

Figure Captions

Figure 12. Schematic of the ramp generation electronics and sensing resistors of the Langmuir probe.

Figure 13. Detail of the Langmuir probe used on the UNH rocket flights.

Figure 14. Modified densitometer circuit diagram.

Figure 15. Picture of the aspect deck showing the mounting of the sensor (on the right) and the sensor electronics (on the left). The baroswitch is at the bottom.

Figure 16. Schematic of the telemetry mixer circuitry.

Figure 17. Schematic of the "mercury" battery deck illustrating the system for electrically holding the relays on during flight.

Figure 18. Sample magnetic signature obtained at the UNH Magnetic Field Observatory. X and Z scales are noted.

Figure 19. Block diagram of the data reduction system used for the magnetometer data.

Figure 20. Block diagram of the system used to handle data from the SCO channels.

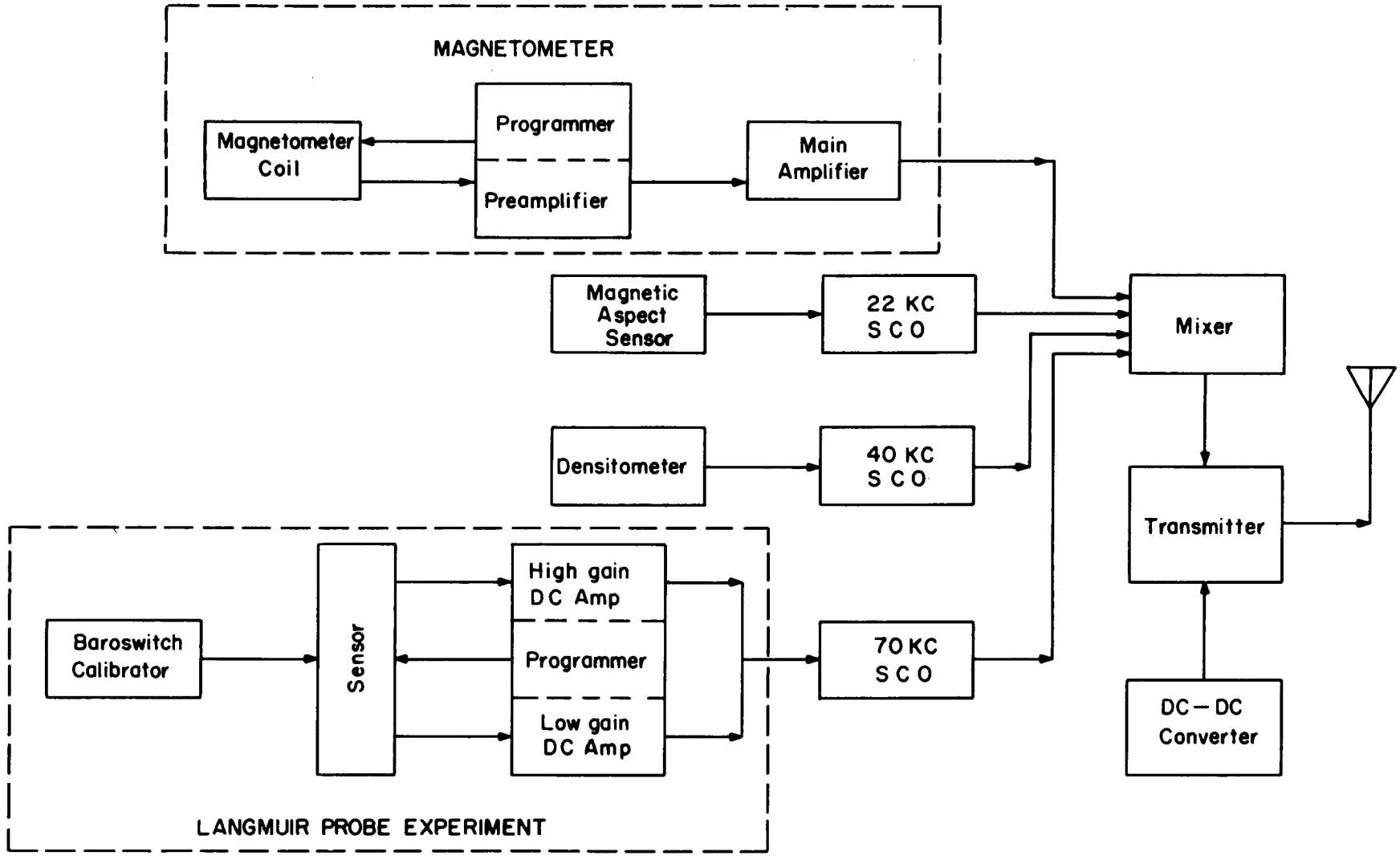

BLOCK DIAGRAM — UNH ROCKET MAGNETOMETER PAYLOAD

Figure 1

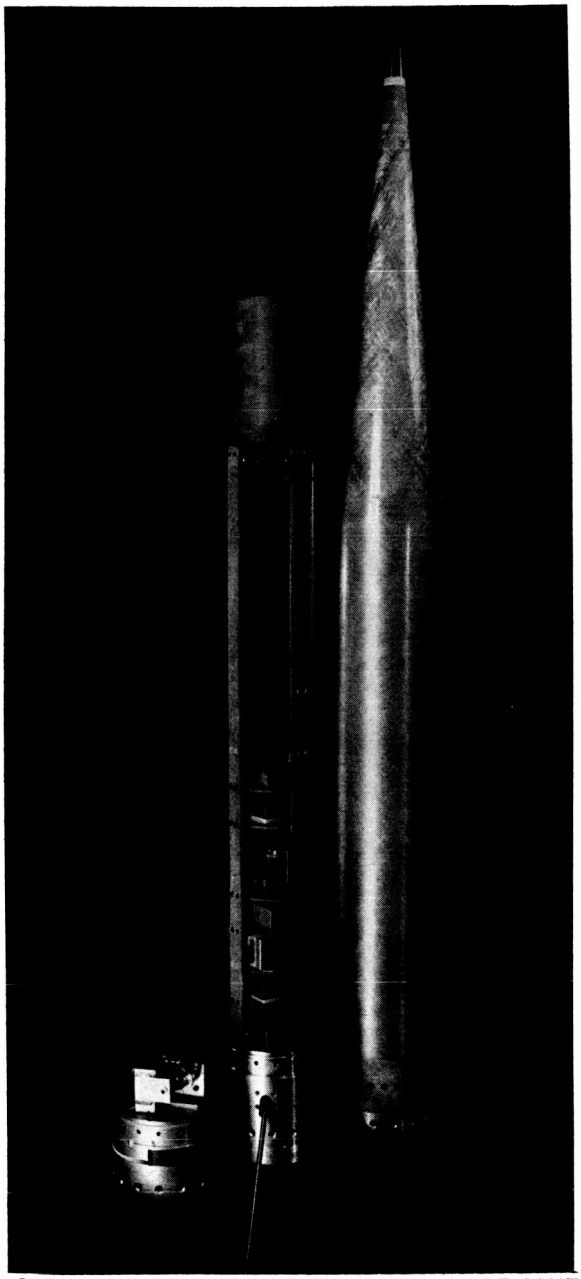

COMPLETE ROCKET PAYLOAD WITH NOSE CONE

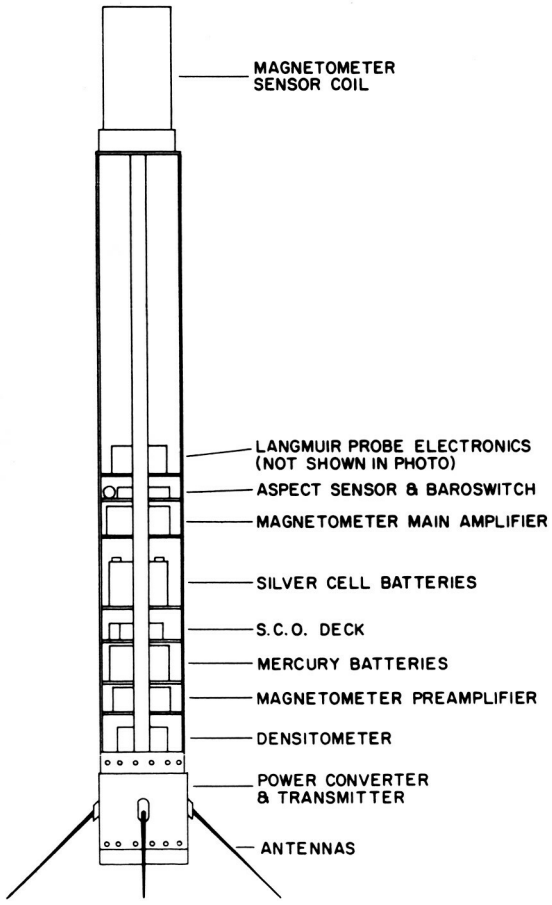

Figure 2

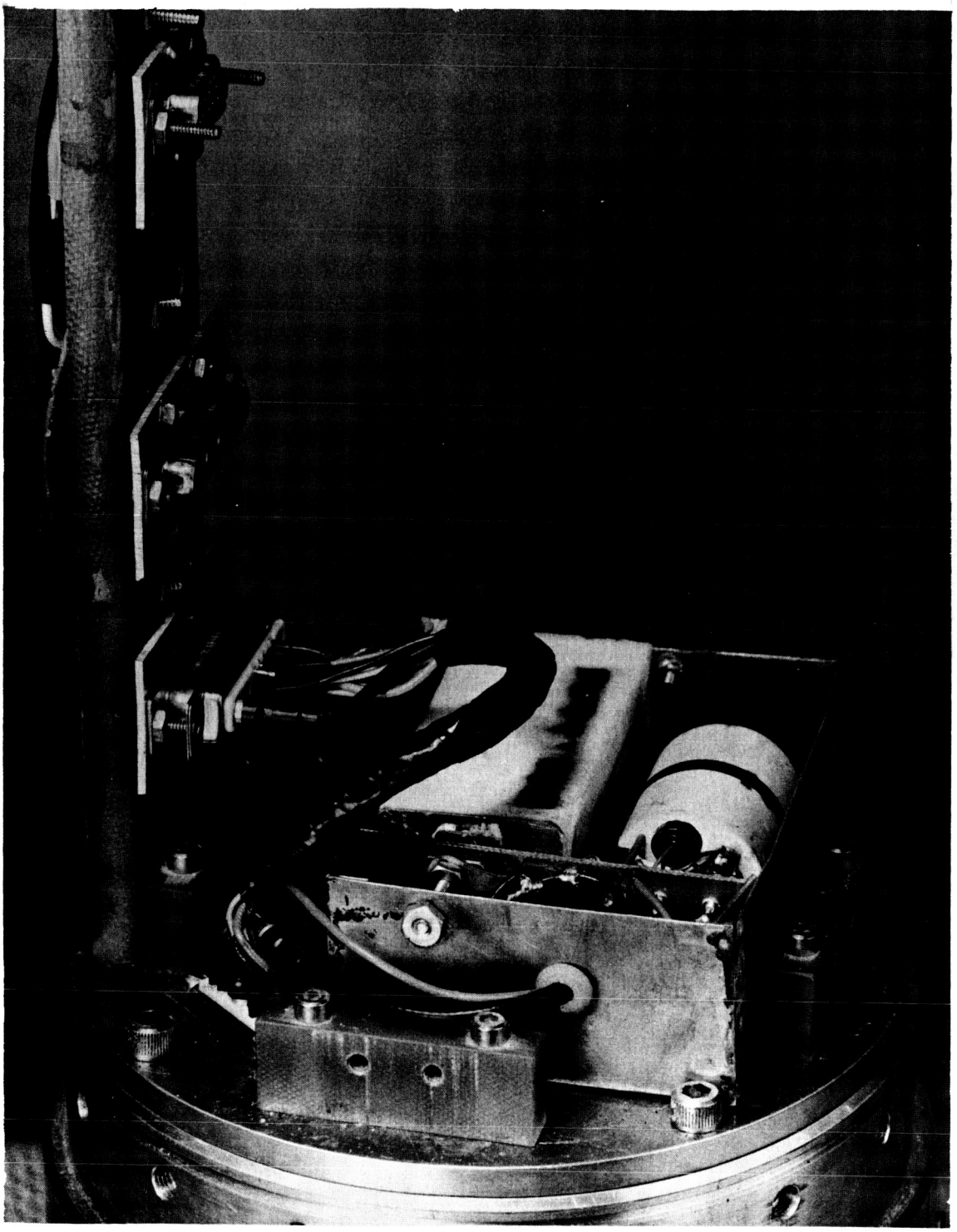

Figure 3

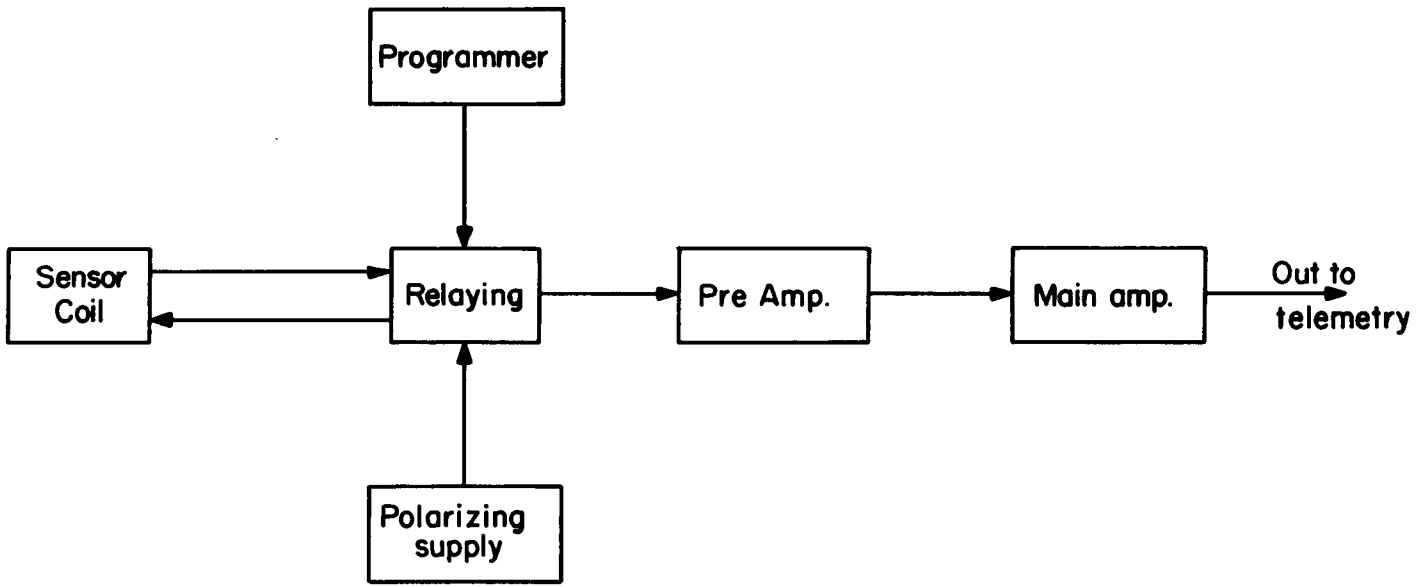

MAGNETOMETER BLOCK DIAGRAM

Figure 4

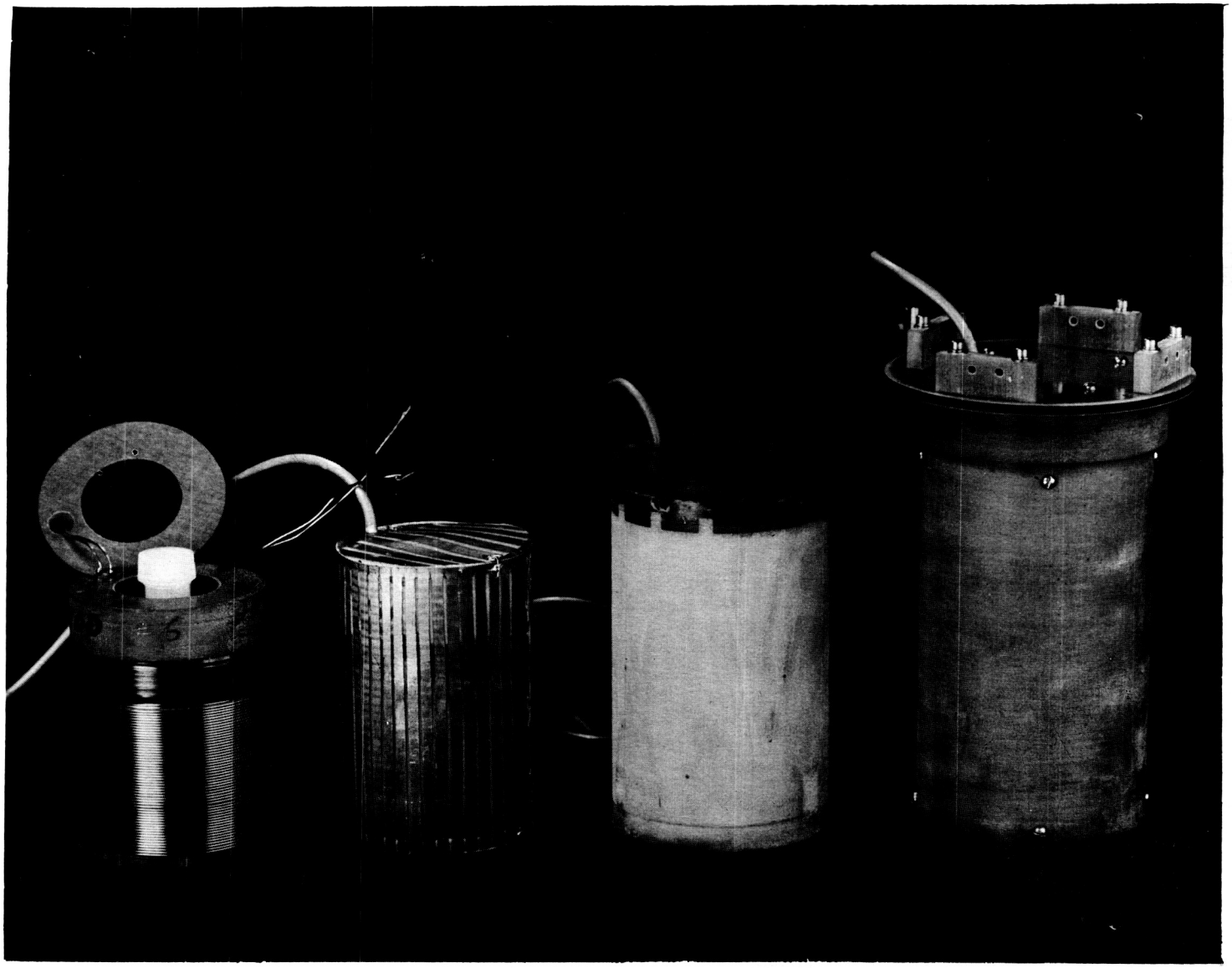

Figure 5

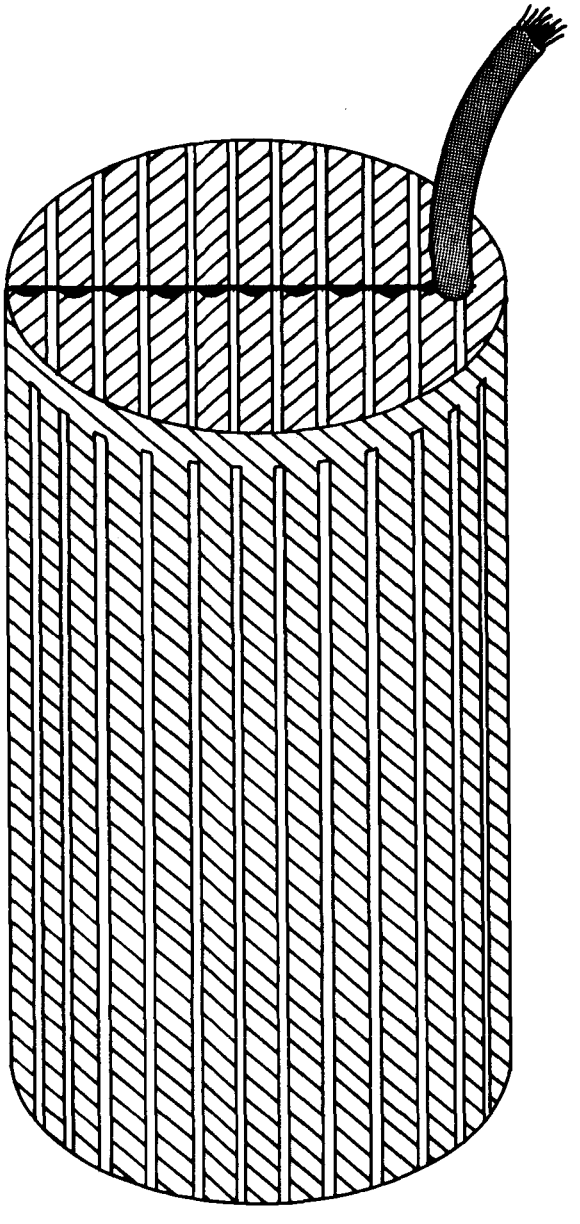

SENSOR WITH ELECTRO STATIC SHIELD

Figure 6

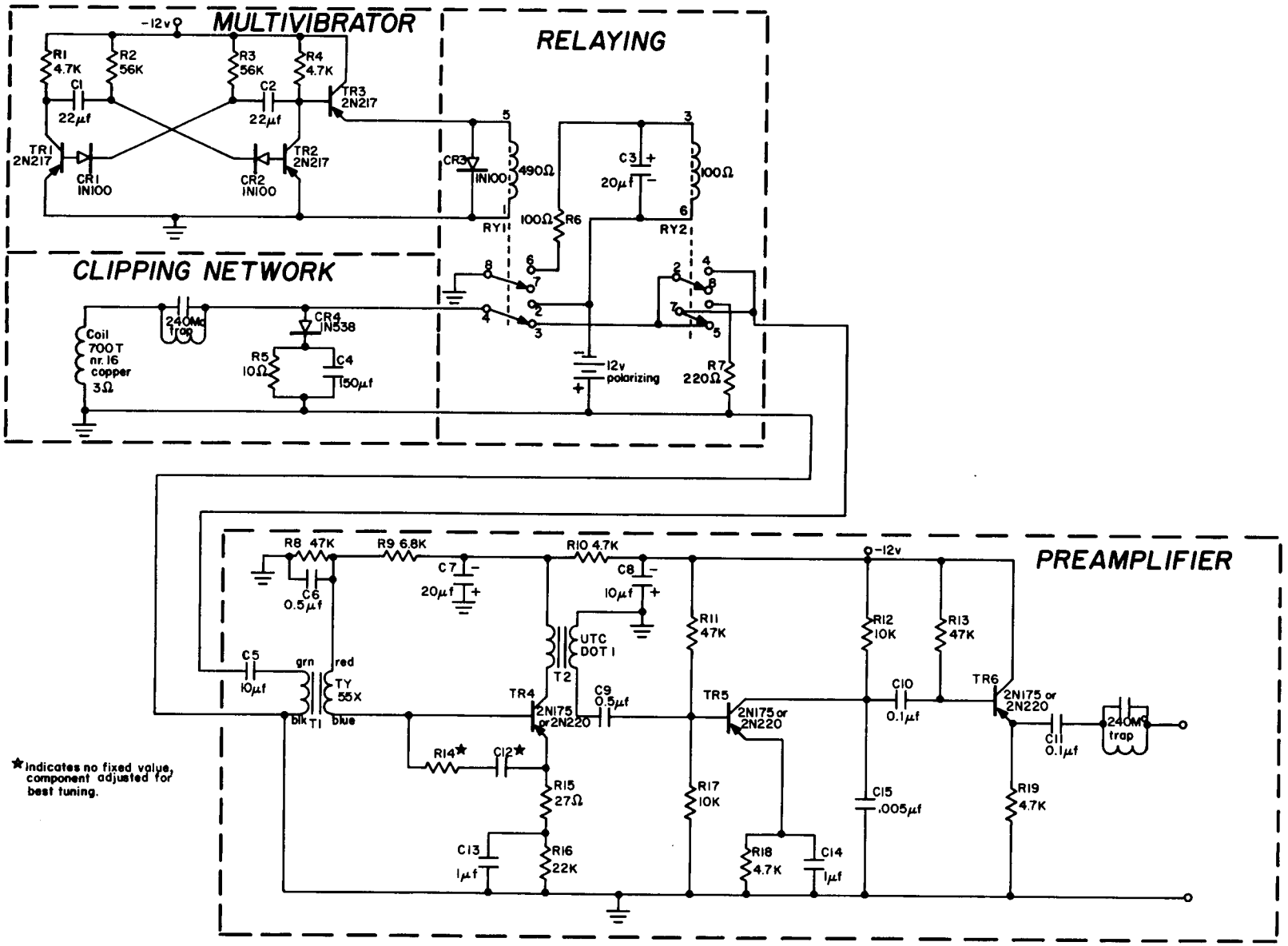
MULTIVIBRATOR
-12v
R1 4.7K
R2 56K
R3 56K
R4 4.7K
C1 22μf
C2 22μf
TR3 2N217
TR1 2N217
TR2 2N217
CR1 IN100
CR2 IN100
RELAYING
CR3 IN100
490Ω
100Ω
C3 20μf
100Ω
100Ω R6
RY1
RY2
CLIPPING NETWORK
Coil 700T nr.16 copper 3Ω
240Mc trap
CR4 IN538
R5 10Ω
C4 150μf
12v polarizing
R7 220Ω
PREAMPLIFIER
R8 47K
R9 6.8K
R10 4.7K
C6 0.5μf
C7 20μf
C8 10μf
C5 10μf
grn
red
TY 55X
blk
T1
blue
T2
UTC DOT 1
TR4 2N175 or 2N220
C9 0.5μf
R11 47K
TR5 2N175 or 2N220
R12 10K
R13 47K
C10 0.1μf
TR6 2N175 or 2N220
C11 0.1μf
240Mc trap
R14★
C12★
R15 27Ω
C13 1μf
R16 22K
R17 10K
R18 4.7K
C14 1μf
C15 .005μf
R19 4.7K
★Indicates no fixed value, component adjusted for best tuning.

Figure 7

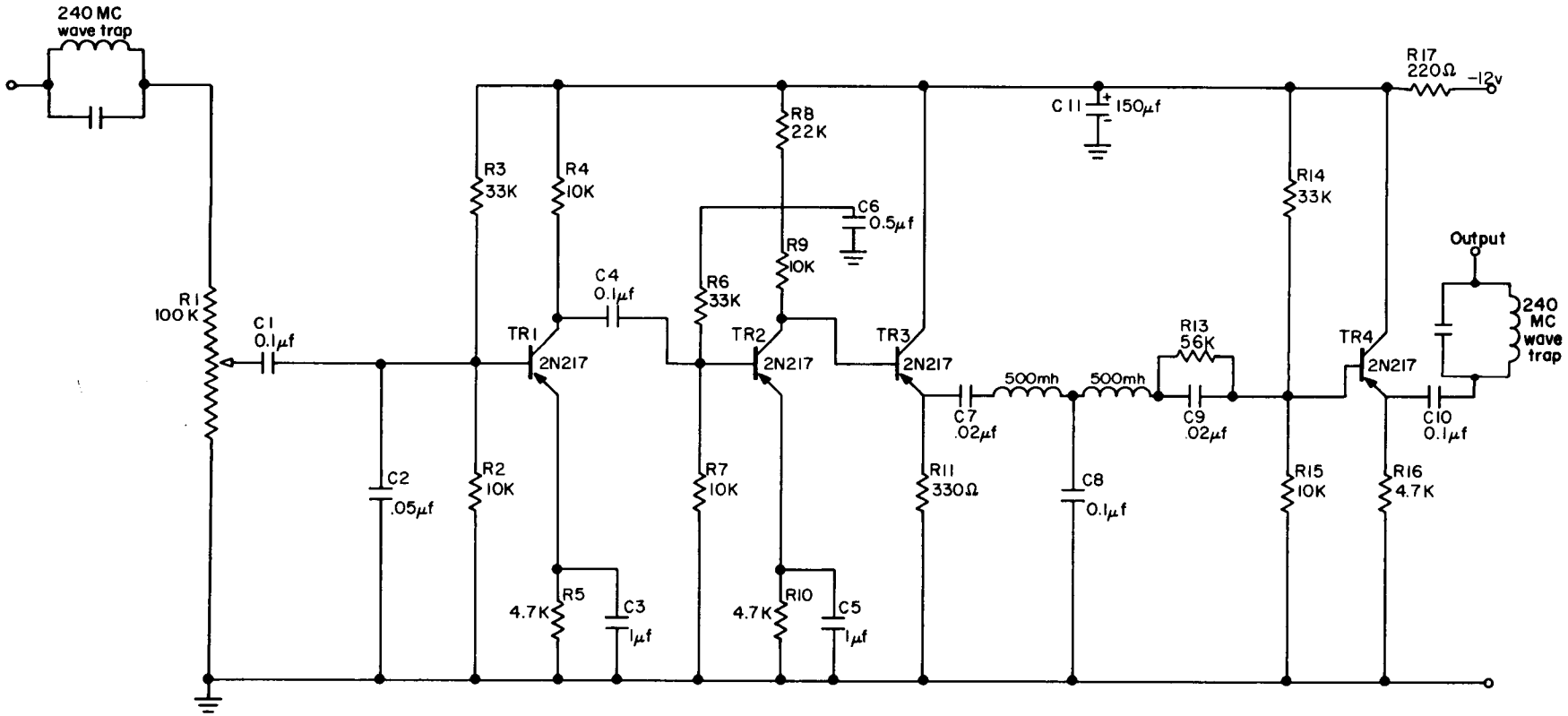

MODIFIED MAIN AMPLIFIER

Figure 8

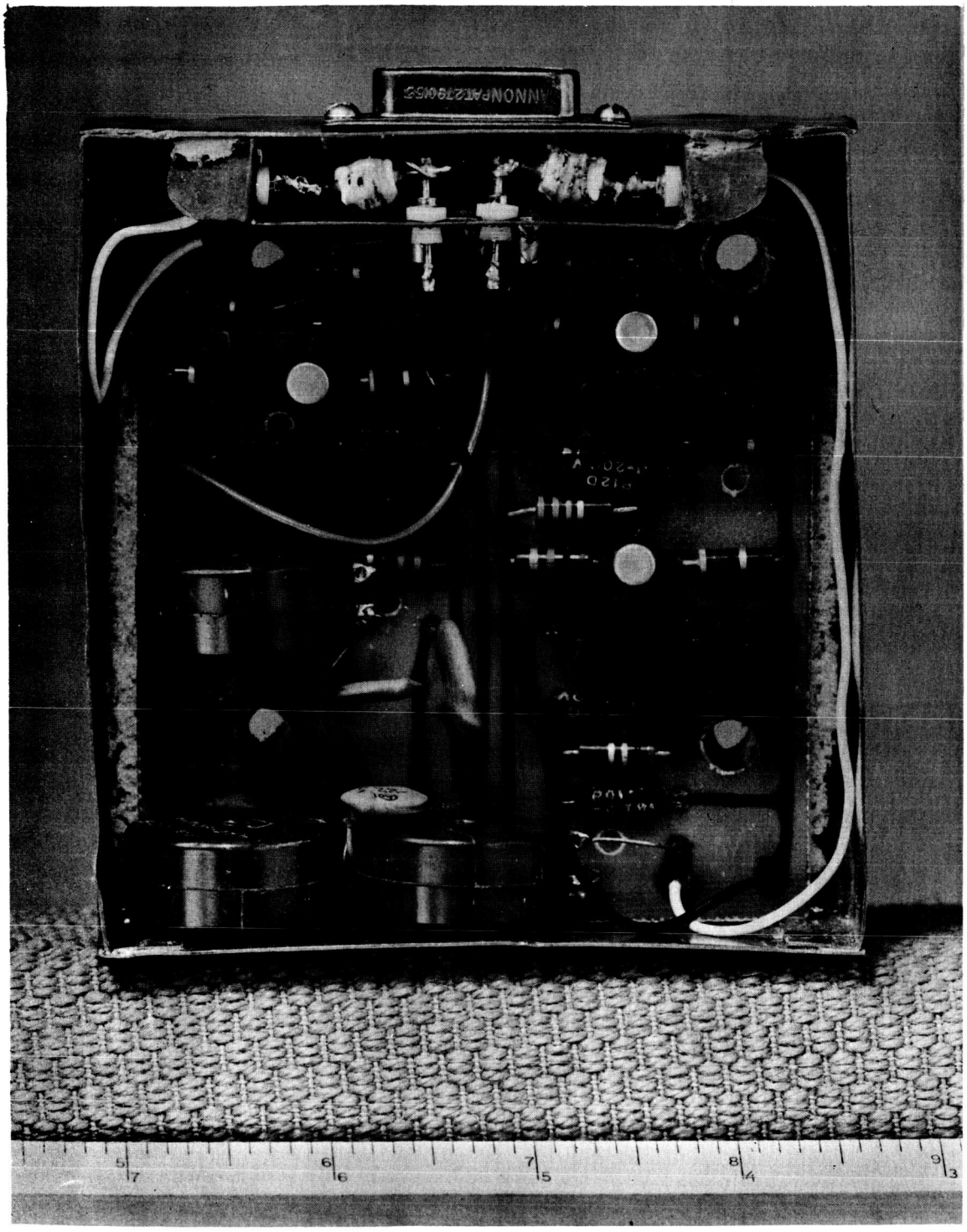

Figure 9

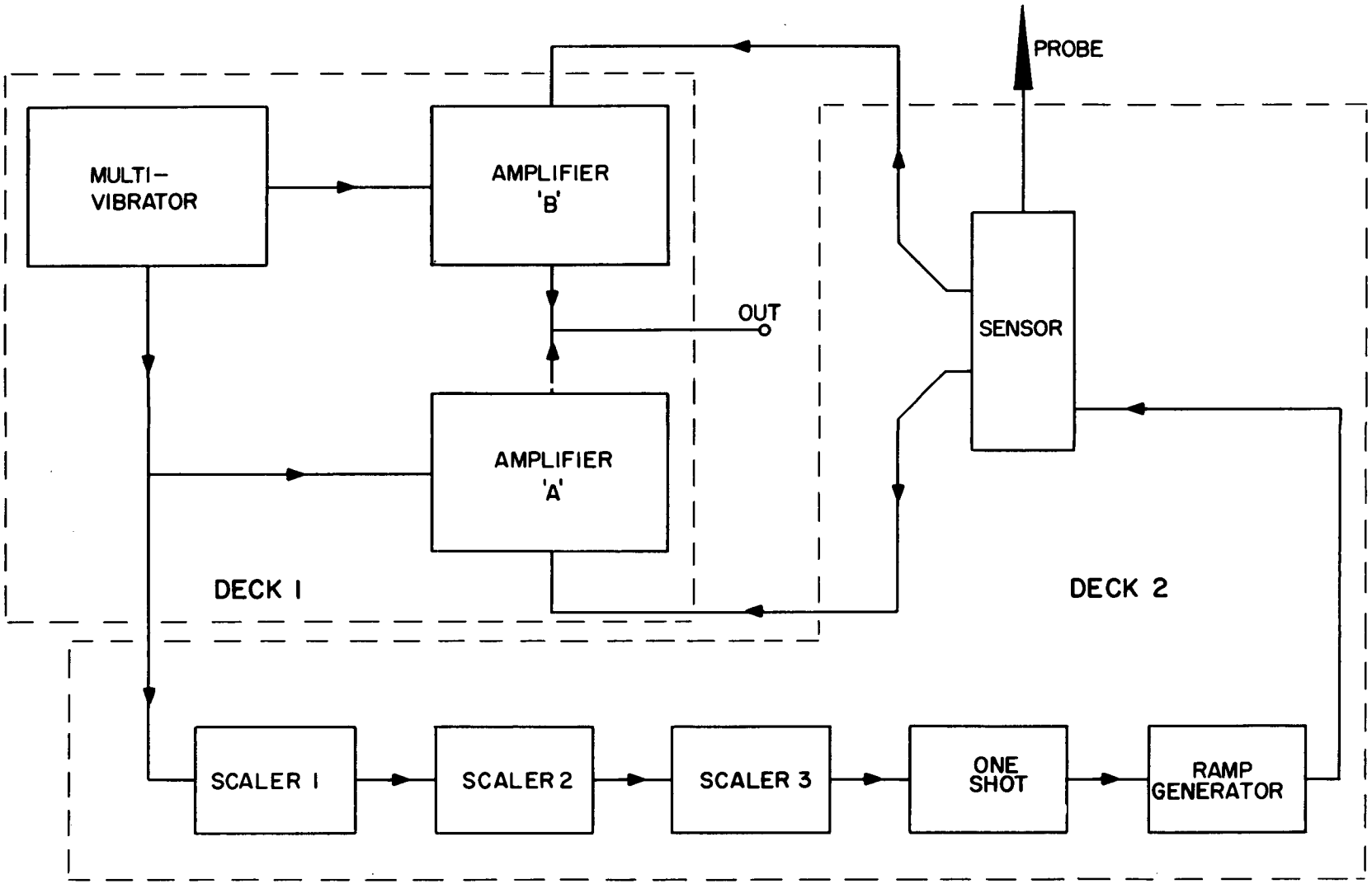

LANGMUIR PROBE BLOCK DIAGRAM

Figure 10

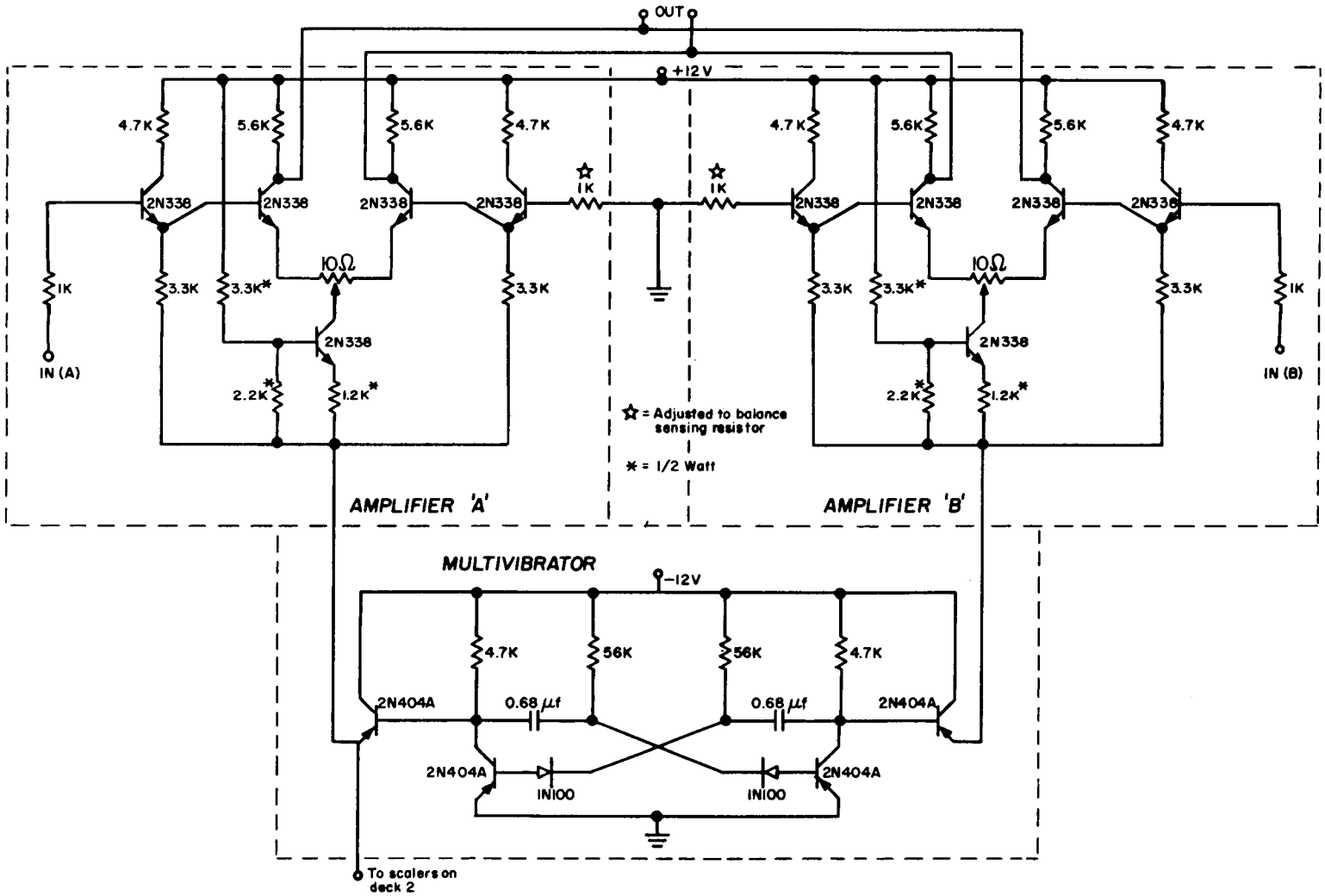

CIRCUIT DIAGRAM — DECK 1

Figure 11

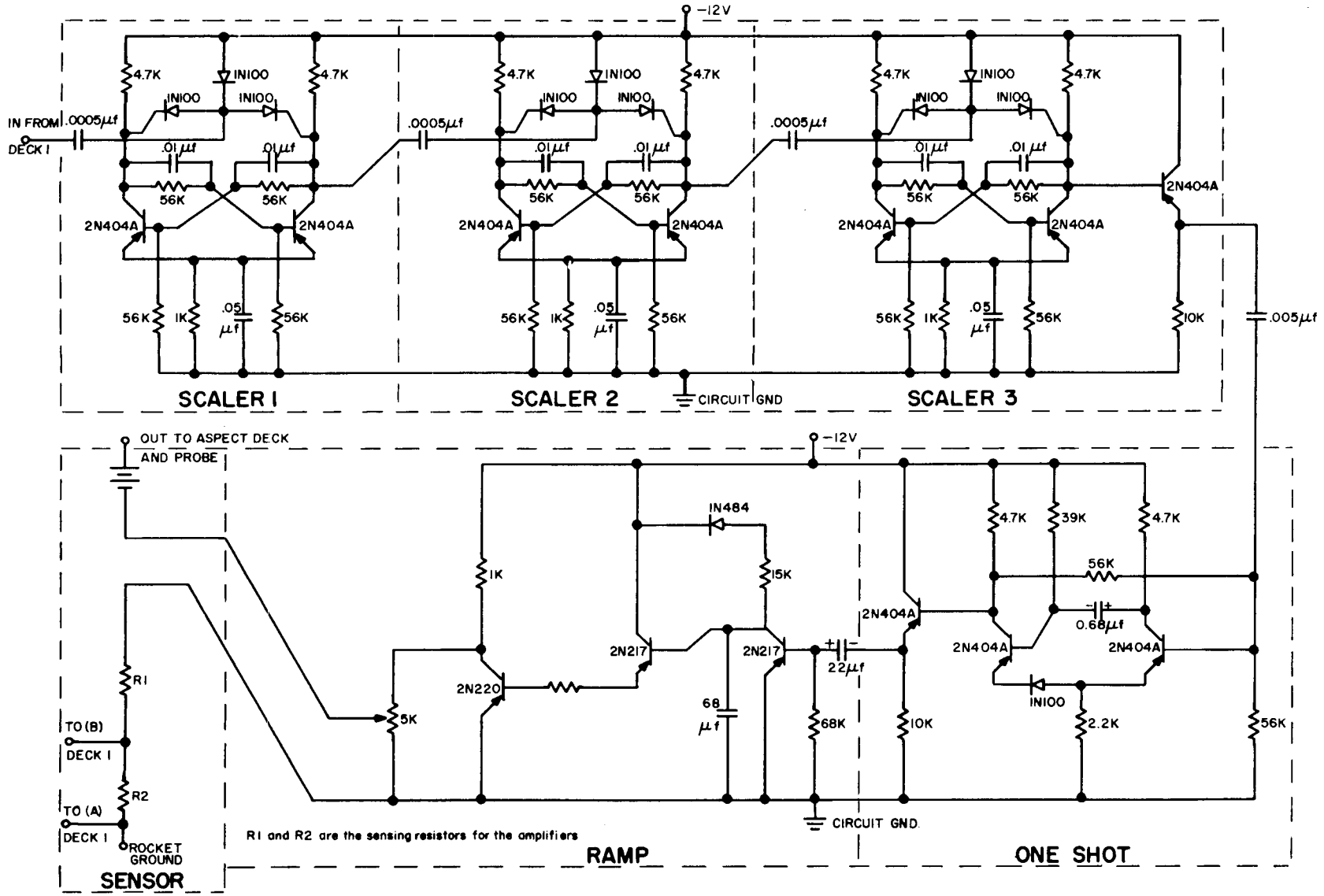

CIRCUIT DIAGRAM—DECK 2

Figure 12

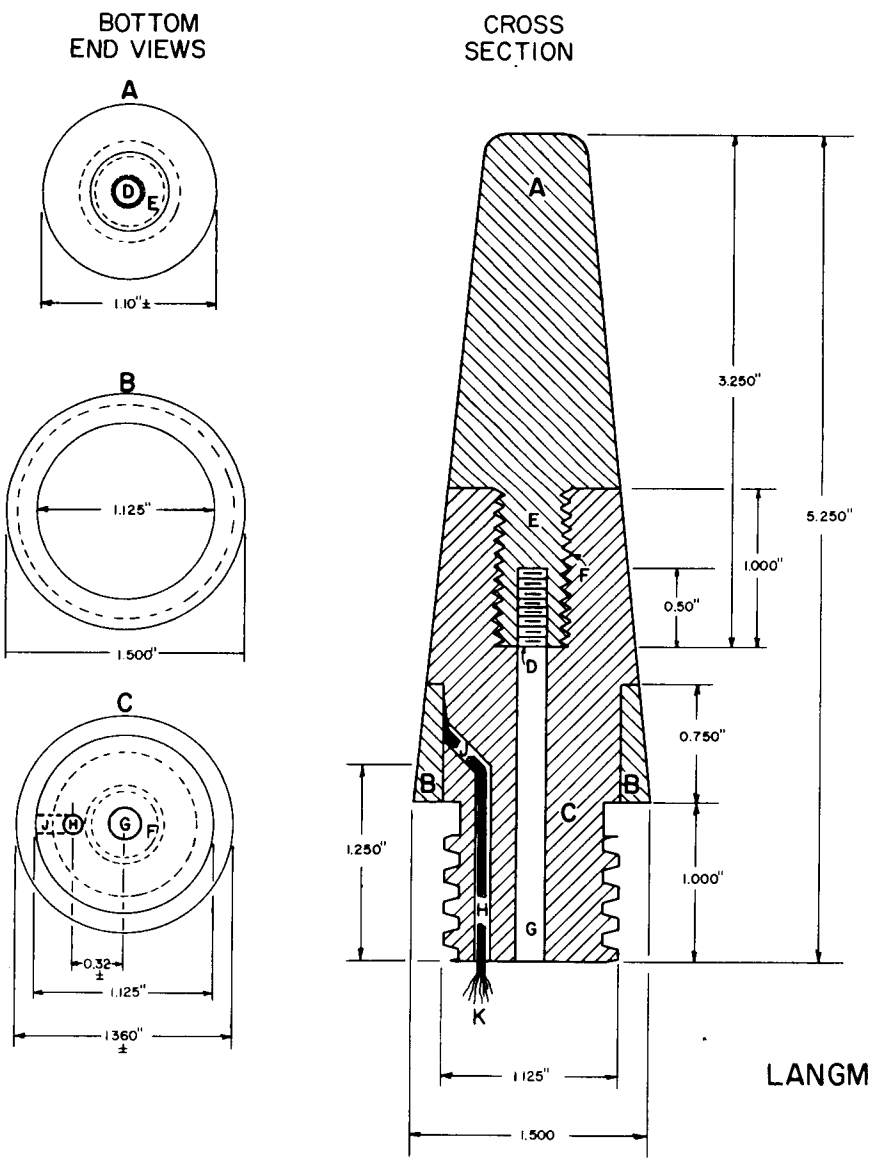

MATERIALS:

Nr. 347 stainless steel (ss) & teflon.

KEY:

A. SS nose, taper 2.50" per foot.
B. SS ferrule, taper 2.50" per foot.
C. Teflon base, taper 2.50" per foot.
D. Hole in SS nose, tapped 10-32, 0.50" deep.
E. SS nose threaded 1/2"-13, 1.00" long.
F. Hole in teflon base tapped 1/2"-13, 1.00" deep.
G. Hole in teflon base, nr. 11 drill.
H. Hole in teflon base, nr. 38 drill, 1.25" deep.
J. Hole in teflon base, nr. 38 drill at 45° to meet hole "H".
K. Nr. 16 stranded copper wire thru hole "H-J", stripped 1/2" at top, and squeezed between ferrule "B" and base "C" for electrical contact.

Bottom of base "C" threaded ACME Nr. 1.

LANGMUIR PROBE ASSEMBLY

Figure 13

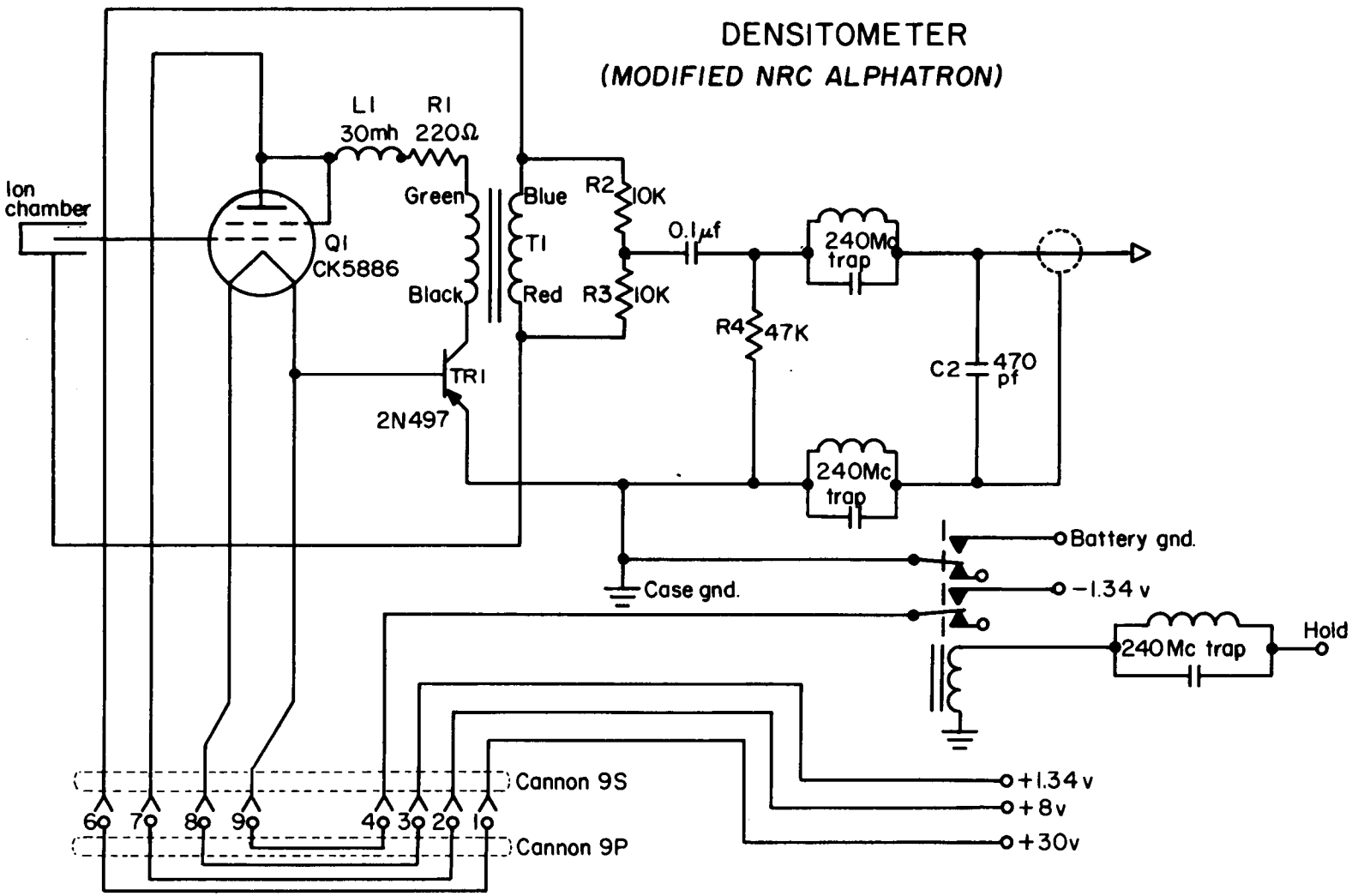
DENSITOMETER
(MODIFIED NRC ALPHATRON)
L1
30mh
R1
220Ω
Ion chamber
Q1
CK5886
Green
Black
Blue
T1
Red
R2
10K
R3
10K
0.1μf
240Mc trap
R4
47K
C2
470 pf
TR1
2N497
240Mc trap
Battery gnd.
Case gnd.
-1.34 v
240Mc trap
Hold
Cannon 9S
Cannon 9P
6
7
8
9
4
3
2
1
+1.34 v
+8v
+30v

Figure 14

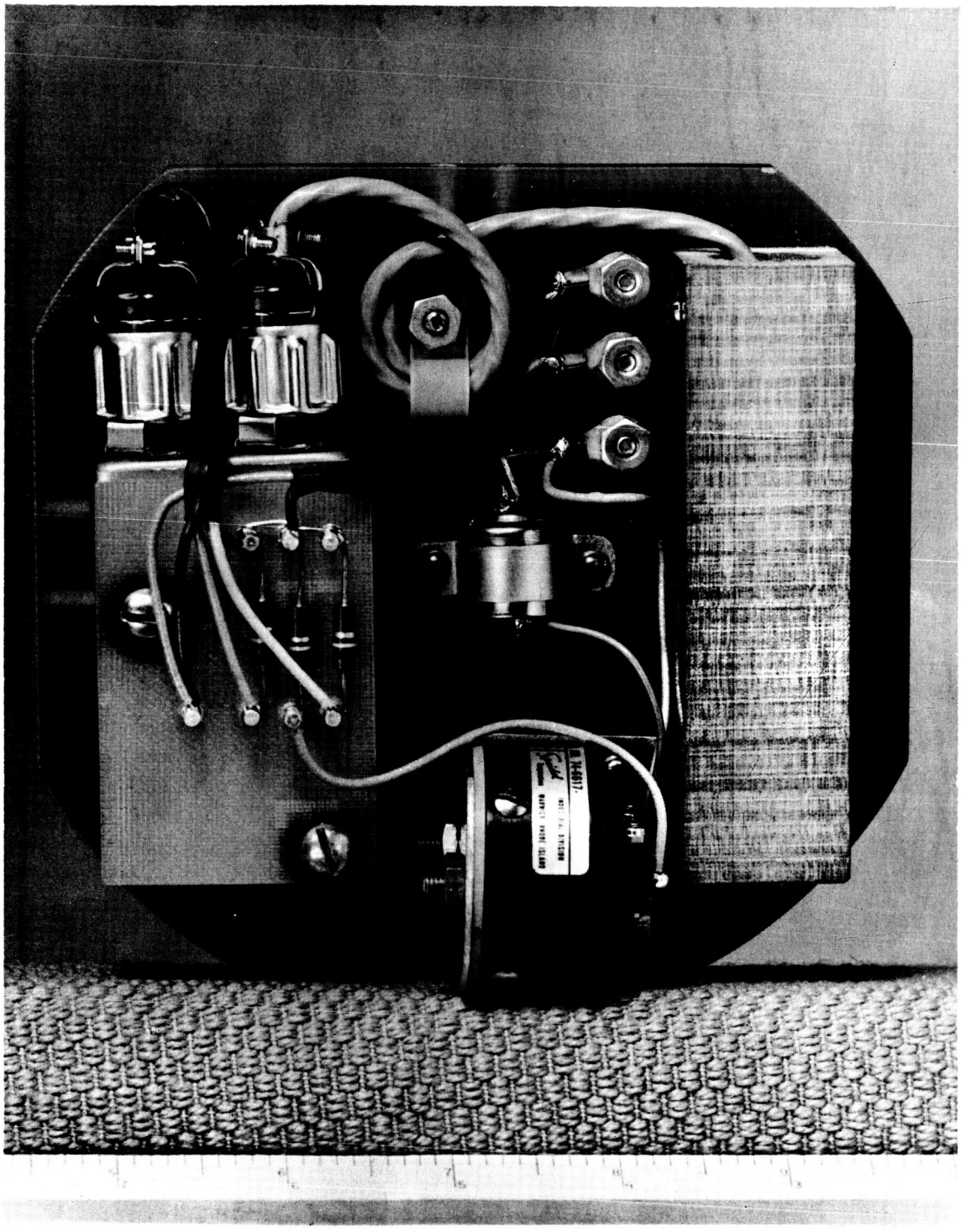

Figure 15

MIXER PLUG-IN SCHEMATIC

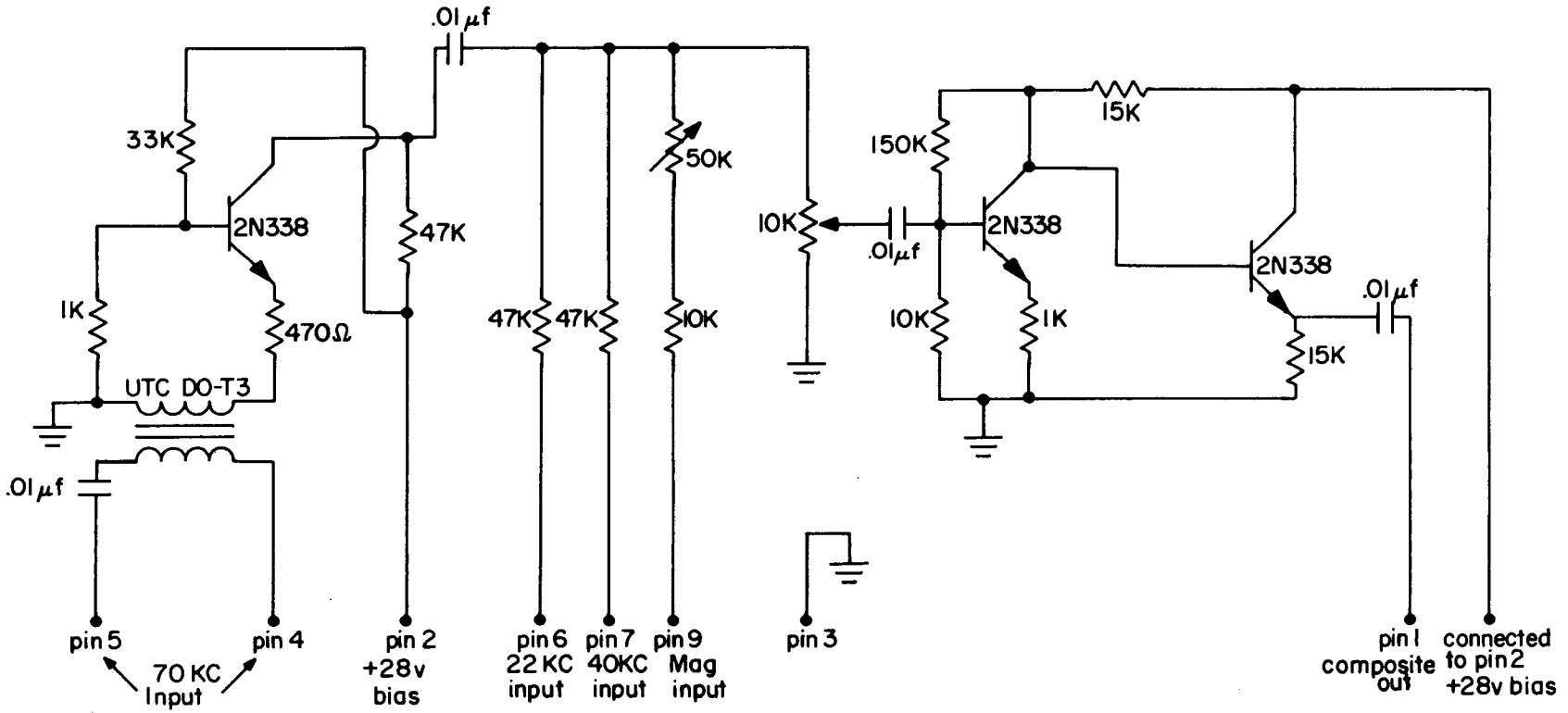

PLUG IS CANNON DEM 9 PNMB

Figure 16

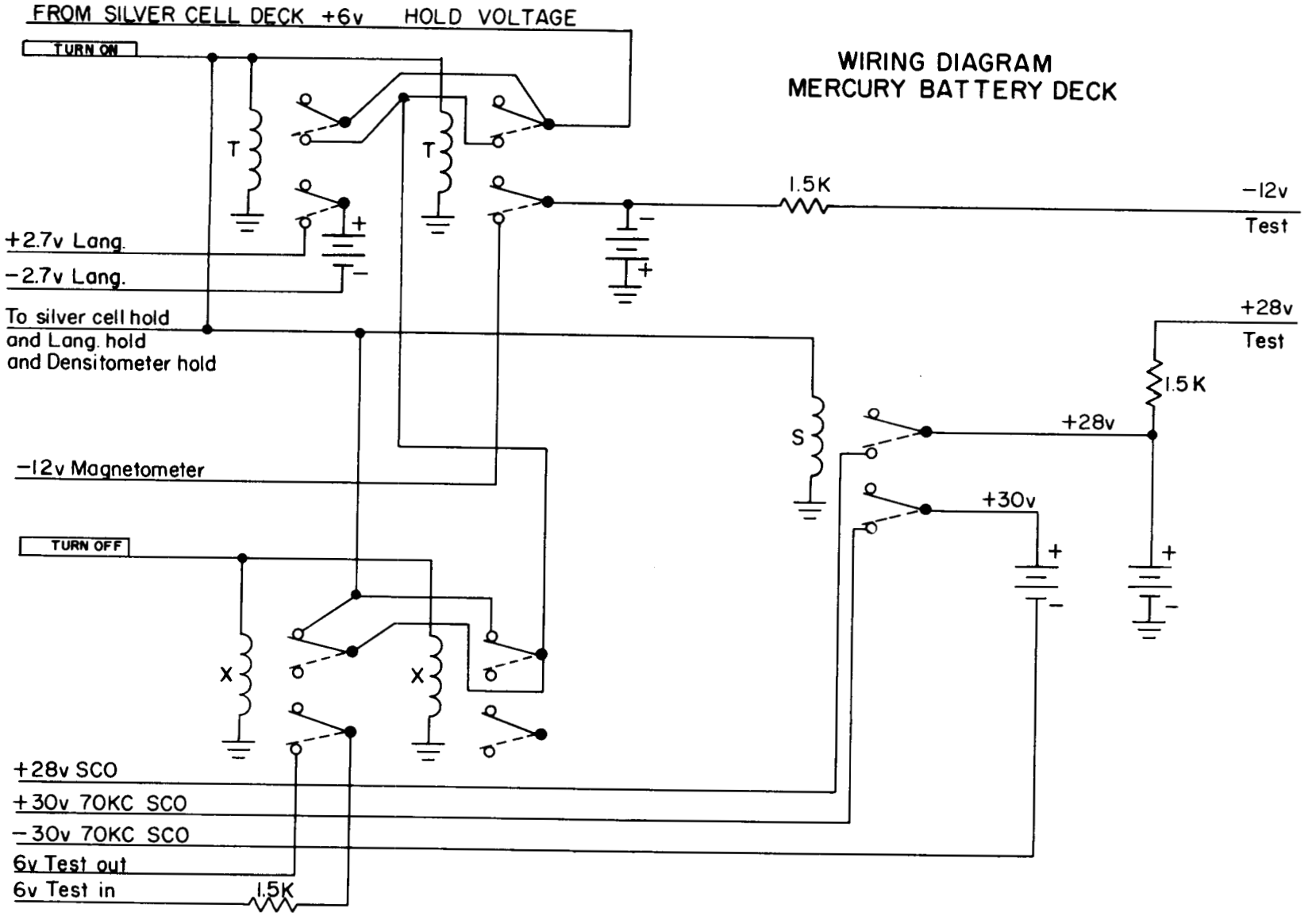
FROM SILVER CELL DECK +6v HOLD VOLTAGE
TURN ON
WIRING DIAGRAM
MERCURY BATTERY DECK
T
T
1.5K
−12v
Test
+2.7v Lang.
−2.7v Lang.
To silver cell hold
and Lang. hold
and Densitometer hold
+28v
Test
1.5K
S
+28v
−12v Magnetometer
+30v
TURN OFF
X
X
+28v SCO
+30v 70KC SCO
−30v 70KC SCO
6v Test out
6v Test in
1.5K

Figure 17

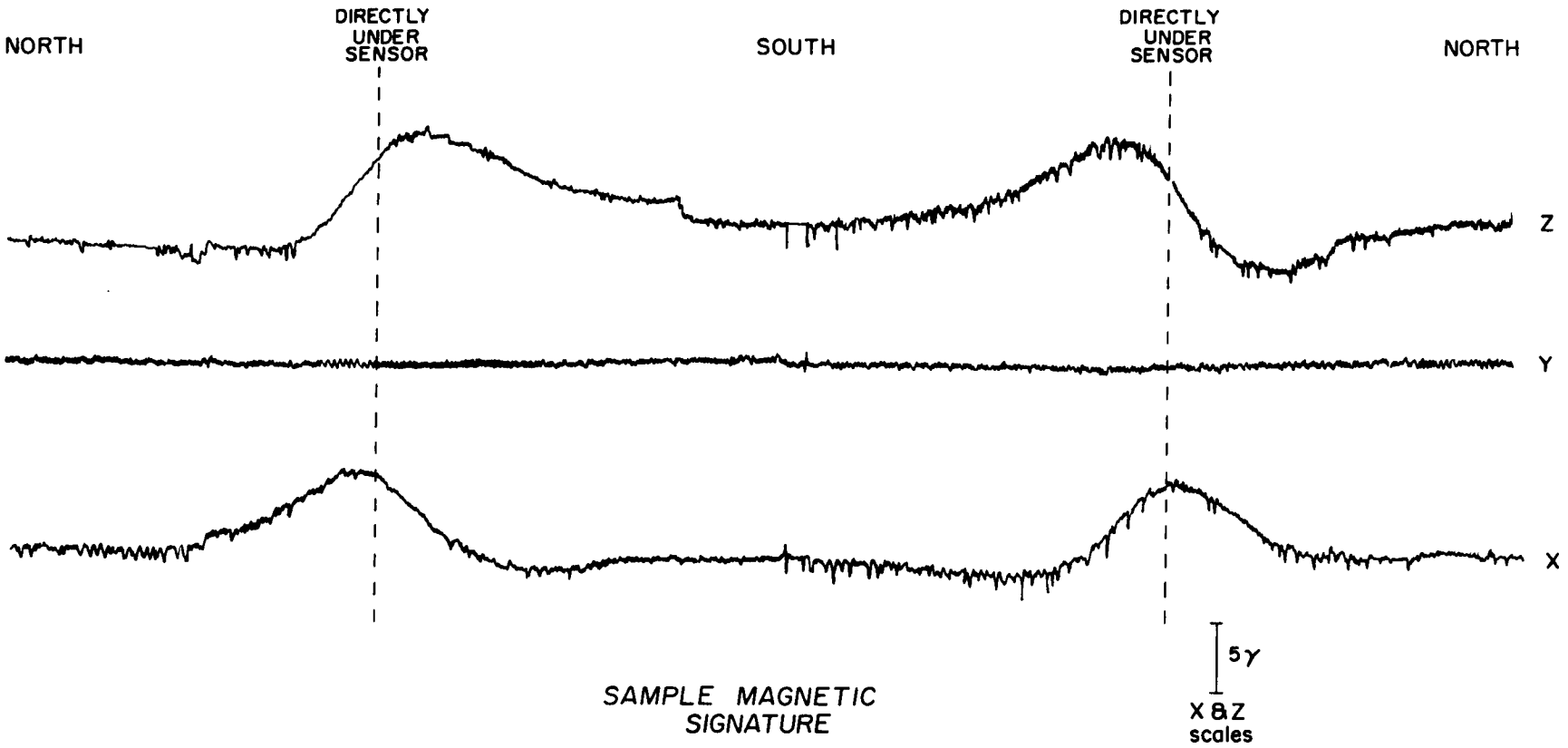
NORTH
DIRECTLY UNDER SENSOR
SOUTH
DIRECTLY UNDER SENSOR
NORTH
Z
Y
X
5γ
X & Z scales
SAMPLE MAGNETIC SIGNATURE

Figure 18

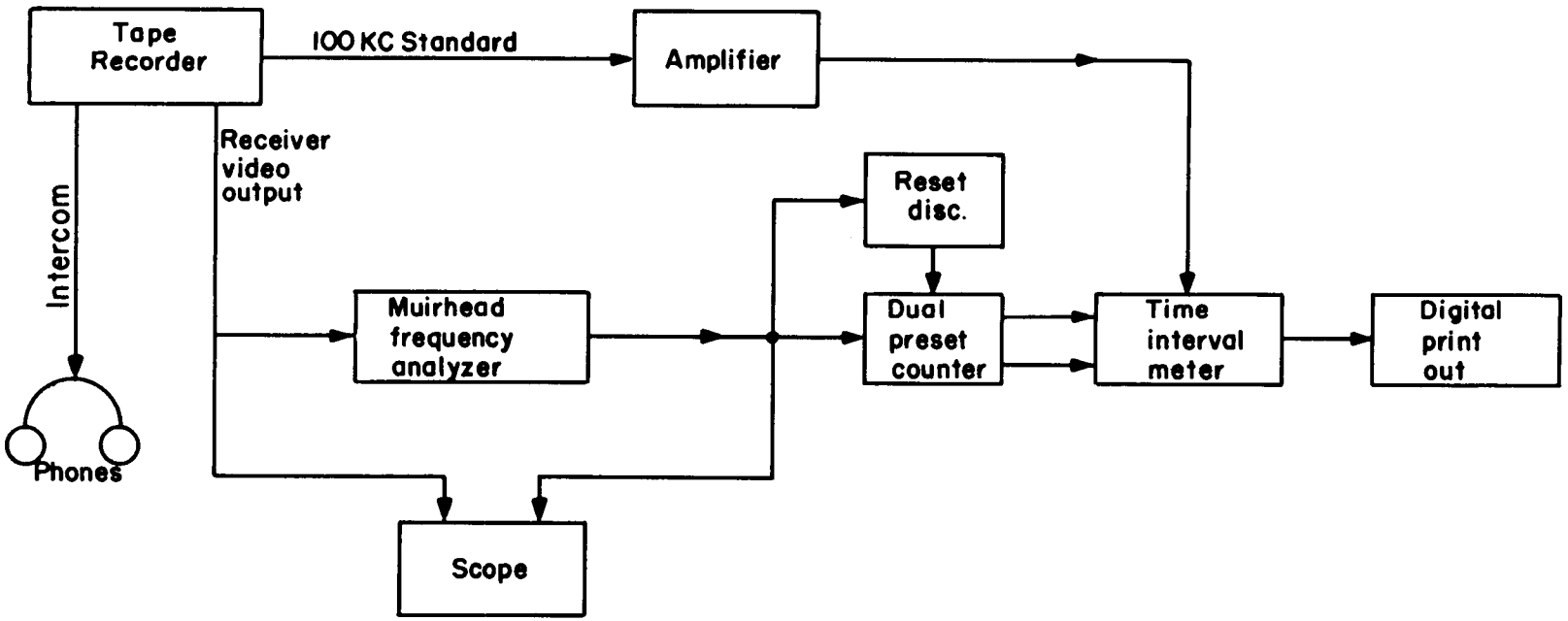

DATA READ OUT SET UP — MAGNETOMETER

Figure 19

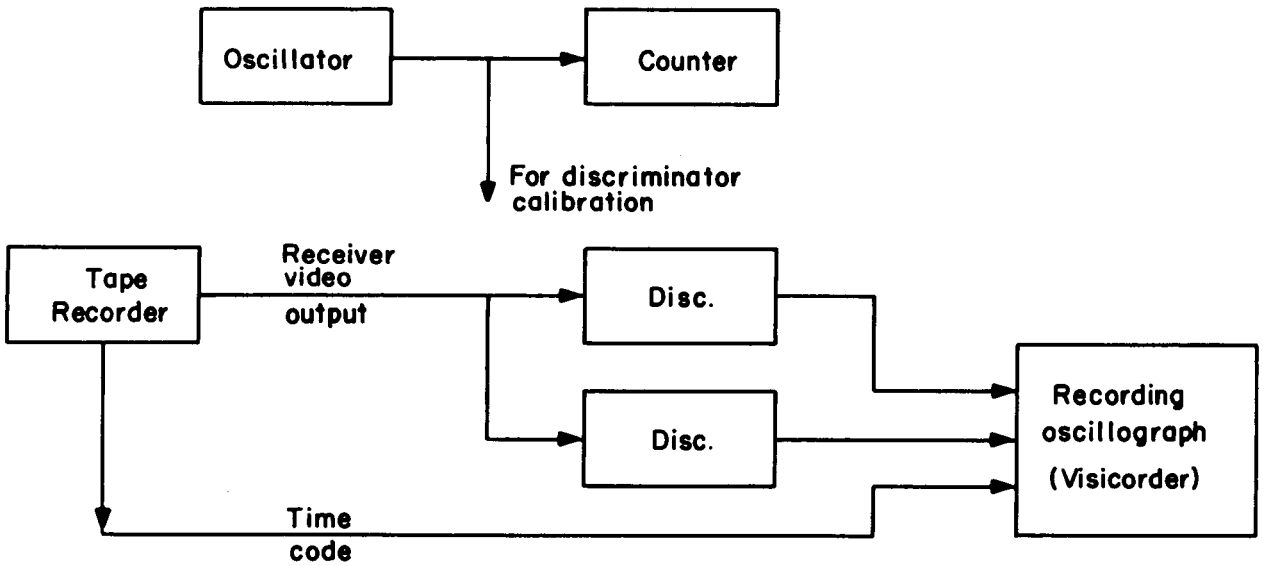

DATA READ OUT SET UP —— SUB-CARRIER CHANNELS

Figure 20